THE UNIVERSITY OF ALBERTA

EXCITON INDUCED PHOTOCONDUCTIVITY IN Cu_2O

by

SYED MUSTAFA JAMAL

A THESIS

SUBMITTED TO THE FACULTY OF GRADUATE STUDIES

IN PARTIAL FULFILMENT OF THE REQUIREMENTS FOR THE DEGREE OF

MASTER OF SCIENCE

DEPARTMENT OF PHYSICS

EDMONTON, ALBERTA

NOVEMBER, 1966

UNIVERSITY OF ALBERTA

FACULTY OF GRADUATE STUDIES

The undersigned certify that they have read, and recommend to the Faculty of Graduate Studies for acceptance, a thesis entitled "EXCITON INDUCED PHOTOCONDUCTIVITY IN Cu_2O", submitted by Syed Mustafa Jamal in partial fulfilment of the requirements for the degree of Master of Science.

ABSTRACT

Photoconductivity measurements were performed on high resistivity single crystals of Cu_2O at liquid nitrogen temperature. Observations were taken with sample having natural surface as well as with surface etched by nitric acid. The sample was heated in vacuo at $150^{\circ}C$ and $950^{\circ}C$ and at $150^{\circ}C$ in air. Structure in the photoconductivity curve was correlated to the exciton lines in yellow, green and blue series. Maxima of photoconductivity was observed corresponding to exciton lines in yellow and green series whereas a minima of photoconductivity was observed for exciton line in the blue region. No change from maxima to minima or vice versa was observed in photoconductivity by different surface and heat treatment of the sample. The conductivity and activation energies of the samples changed with the surface and heat treatments of the samples. Negative photoconductivity was not observed for electric fields upto 2 KV/cm applied across the sample.

The photoconductivity in the exciton lines has been explained on the basis of the dissociation of excitons on defects or localised impurity centres. The conductivity data are interpreted on the basis of simple band theory. The results have been compared with previous investigations and the difference in results has been explained.

ACKNOWLEDGEMENTS

It is a great pleasure to express my gratitude to my supervisor, Dr.F.L.Weichman, for suggesting this problem and for his assistance and encouragement during the course of this research. The present form of this thesis, to a great extent, was made possible by many of his invaluable suggestions.

I would also like to express my thanks to Dr. S.B.Woods for his assistance in the absence of Dr. F.L.Weichman.

Thanks are also due to Mr.Hank McClung, Mr.Jack Cuthiell and the members of the technical staff of the Physics Department for their help. The author is also indebted to Mr. Peter Alexander for his patient and excellent glass work.

The financial assistance provided by the University of Alberta and the National Research Council is gratefully acknowledged.

TABLE OF CONTENTS

LIST OF FIGURES

CHAPTER I

1.1 Introduction.

Frenkel (1) was the first to recognise the possibility of the existence of excited states in a crystal lattice which are not associated with the appearance of electrical conductivity in the crystal. This excitation of the lattice may be caused by the absorption of a light quantum such that the excited state consists of an electron-hole pair coupled together in a hydrogen-atom-like structure which Frenkel called an exciton. The ideas concerning excitons found further development in the theoretical papers by Peierls (2), Wannier (3), Mott (4) and others. Experimental evidence for the actual existence of excitons were found from the structures observed in the fundamental absorption edge of the optical absorption spectra of Cu_2O observed independently by Gross and Karryev (5) and Hayashi (6).

Excitons being electrically neutral, cannot carry a current through a crystal. However, since they allow the crystal to absorb energy and are able to transport energy, excitons may play an important role in the production of

charge carriers in photoconductivity in a number of ways, e.g., interaction with phonons, exciton dissociation by static impurities or crystal defects, collision between excitons, etc. Fine structure obtained in the photoconductivity spectra of some of the crystals were thus attributed to the existence of excitons. Correspondence between the structure observed for optical absorption and the spectral structure in photoconductivity curves was first obtained experimentally by Gross et al (7) in CdS and HgI_2. Similar correspondence has now been observed in a large number of crystals. Either a maximum or a minimum of photoconductivity is observed at photon energies which coincide with the energies at which absorption maxima, due to exciton formation, are found in optical absorption spectra. Such experiments for Cu_2O were carried out by Gross and Pastrnyak (8), Apfel and Portis (9) and many others.

Studies with Cu_2O and other crystals showed that treatments like etching, polishing and grinding, heating and quenching, temperature changes on the same crystal, and frequency of modulation of incident light produced profound changes in the nature of the fine structure in their photoconductivity curves.

Due to the fact that exciton induced photoconductivity in different spectral regions is very sensitive to the nature of the specimen surface, impurity contents, defects, structures and different treatments given to the crystal, the present work was therefore undertaken with the following objectives:

1. To study the structure, caused by excitons, in the photoresponse of high resistivity single crystals of Cu_2O.
2. To study the effects of outgassing these crystals at different temperatures on the structure of the photoresponse curve.
3. To study the effect of etching the crystal surface, on the fine structure of the photoconductivity curve.

The last two points have been studied by Gross and Pastrnyak (8) and Coret and Nikitine (37) but on very low resistivity and polycrystalline material.

CHAPTER II

THEORY

2.1 Electrical Conductivity.

The electrical properties of metals, semiconductors and insulators can be explained by means of the band theory of solids. According to this theory, the electrons in a solid belong to the whole solid rather than to the individual atoms constituting the solid. The energy states of such electrons in the solid consist of allowed energy bands separated by forbidden regions whose width varies from substance to substance. The uppermost band which is completely filled by electrons is called the valence band and the next higher band partially filled or empty is called the conduction band. Due to the partial occupation of the conduction band, the electrons in this band are free to move under the action of an electric field and therefore can cause electrical conductivity. On the other hand, the valence band is completely full and electrons in this band cannot take part in electrical conductivity unless they are excited to the conduction band by providing them sufficient energy to overcome the energy gap. Electrons when excited from the valence band leave holes in the valence band. Both electrons and holes are able to accept energy under the action of an external

field and give rise to electrical conductivity. The difference between metals, semiconductors and insulators lies in the occupation of the energy bands and the width of the forbidden energy gap. Metals owe their high conductivity, either due to the partial occupation of the conduction band or to the overlapping of different energy bands in which case the energy gap vanishes. In semiconductors and insulators the conduction band is completely empty at absolute zero of temperature. The difference between semiconductors and insulators is only a qualitative one, in that the magnitude of the energy gap for an insulator is higher.

Semiconductors at absolute zero of temperature behave as insulators. As the temperature increases, electrons will be thermally excited from the valence band to the conduction band creating holes in the valence band. The conductivity will thus result as explained earlier. The conductivity resulting from such band-to-band transitions is called "intrinsic conductivity." The model of an intrinsic semiconductor is shown in Figure 1.

If n_e and n_h are the numbers of electrons and holes per unit volume and μ_e and μ_h be their respective mobilities, defined as velocity per unit electric field, the intrinsic conductivity is then given by

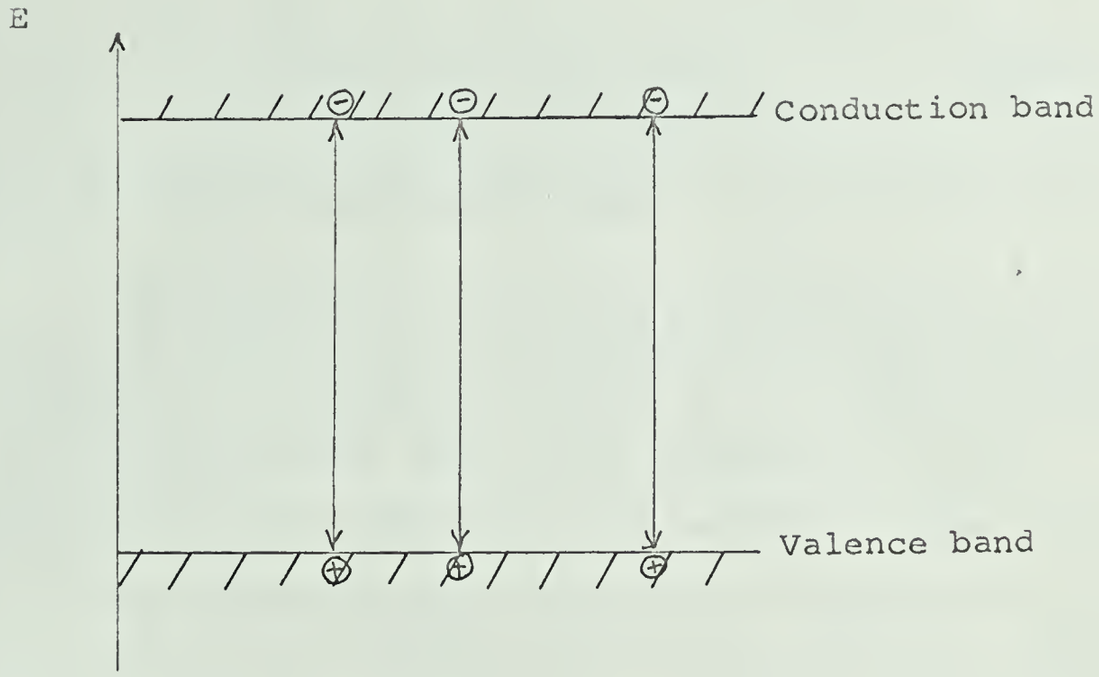

Figure.I. Model of an intrinsic semiconductor.

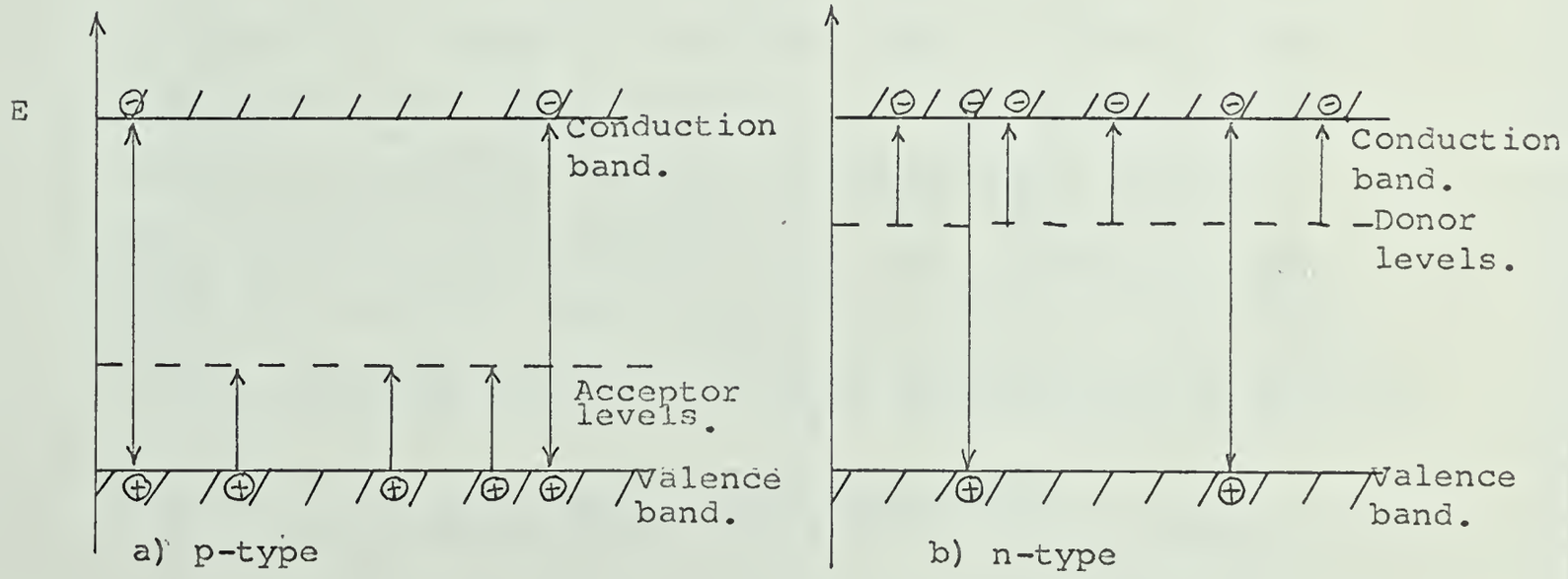

Figure.2. Model of n-type and p-type semiconductor.

$$\sigma = (n_e \, e \, \mu_e + n_h \, e \, \mu_h) \qquad (2.1)$$

where e is the electronic charge.

The density of free electrons and holes is obtained by multiplying the number of states in the energy interval dE in the appropriate band by the probability of its occupation "f" and summing over all possible states in the band. The probability of occupation of an energy level "E" by electrons at any temperature "T" is given by the Fermi function

$$f = \frac{1}{e^{\frac{E-E_F}{KT}} + 1} \qquad . \qquad (2.2)$$

E_F denotes the energy at the Fermi level. The Fermi level is defined as the energy level at which the probability of occupation is exactly one half. Assuming that the Fermi level lies more than about $4KT$ above the valence band and below the conduction band, calculations show that the density of free electrons and holes to a good approximation is given by

$$n_e = 2(2\pi \, m_e^* KT/h^2)^{3/2} \, e^{(E_F-E_c)/KT} \qquad (2.3)$$

$$n_h = 2(2\pi \, m_h^* KT/h^2)^{3/2} \, e^{(E_V-E_F)/KT} \qquad (2.4)$$

where m_e^* and m_h^* are the effective masses of the electrons and the holes respectively which are different from their masses in the free state due to interactions with the lattice.

E_c and E_v are the energies at the conduction and valence band edges and $E_g = E_c - E_v$. For intrinsic semiconductors, $n_e = n_h$ and it can be easily shown that

$$n_e = n_h = 2\left(\frac{2\pi KT}{h^2}\right)^{3/2} (m_e^* m_h^*)^{3/4} e^{-E_g/2KT} \qquad (2.5)$$

$$\begin{aligned} \sigma &= 2e(2\pi KT/h^2)^{3/2} (m_e^* m_h^*) e^{-E_g/2KT} (\mu_e + \mu_h) \\ &= \sigma_o e^{-E_g/2KT} \end{aligned} \qquad (2.6)$$

As the mobilities depend on temperature only rather weakly, in fact usually as a power law over an appropriate temperature region, the intrinsic conductivity reflects the exponential dependence of carrier concentration on temperature. The slope of $\log \sigma$ vs $\frac{1}{T}$ curve, thus, should give the value of E_g reasonably well.

Most of the semiconductors, however, owe their conductivity to the presence of certain types of impurities. Such impurities produce localised energy levels in the

forbidden energy gap. Low energy transition of electrons from or to these levels are thus made possible. The conductivity in these crystals is very sensitive to the amount of these impurities and, within certain temperature ranges, is entirely governed by them. Such semiconductors are known as "extrinsic semiconductors."

Extrinsic semiconductors are either (i) n-type or (ii) p-type. In n-type semiconductors the current is carried primarily by electrons excited from impurity levels called "donor levels" which are close to the conduction band. In p-type semiconductors however, current is carried primarily by holes. These holes are created due to the transition of electrons from the valence band to the impurity levels called "acceptor levels" which lie close to the valence band. If both the donor and the acceptor levels are present, the sign of the majority carriers determines the type of semiconductor. Figure 2 shows the model of an n-type and a p-type semiconductor.

Cuprous oxide is known to be a p-type semiconductor. This type of behaviour may be caused by two types of impurities. The most important is one in which positive copper ions are missing from the lattice points they normally occupy. This will produce an excess of negative charges at negative ion

sites by the same amount as the missing positive ions (i.e. Cu^{+} ions). Since the crystal as a whole is electrically neutral, some of the negative ions (O^{--} ions) will lose electrons to get rid of this excess negative charge. That means we will have positive holes at the ion sites which have lost their electrons. When the crystal is in its state of lowest energy, the holes will be trapped in the vicinity of the points where the copper ions are missing. In other words, at the points where copper ions are missing there exist empty states above highest level in the full valence band. At increased temperatures some of these states are filled due to the transition of electrons from the valence band leaving mobile positive holes in the valence band.

The second possibility is the existence of electronegative oxygen atoms in interstitial positions of the lattice. Here it can receive an electron from the full valence band leaving a positive hole there. Thus interstitial oxygen atoms may act as acceptors. It should be noted that n-type conductivity should result in Cu_2O if Cu^{+} ions are in interstitial positions.

For extrinsic semiconductors, the expression for electrical conductivity is found to be of the form

$$\sigma = \sum_{i=1}^{n} A_i \, e^{-E_i/KT} \qquad (2.7)$$

The semiconductor has n-1 impurity levels. E_1 is the activation energy ($E_{g/2}$ in equation 2.6) for intrinsic conductivity and E_i ($i > 1$) are the activation energies for impurity levels. In deriving equation (2.7) we assume that the number of available charge carriers is larger than the number of impurity levels to or from which the excitations take place. Each term in equation (2.7) will be dominant within a certain range of temperature.

If we plot $\log \sigma$ vs $\frac{1}{T}$ we will obtain straight line segments with different slopes from which we can calculate the position of impurity levels in the forbidden energy gap.

Survey of literature.

The electrical conductivity of Cu_2O has been investigated by a number of workers as early as 1932. Results vary greatly because of difference in methods of sample preparation, techniques of measurement, impurity contents, crystalline structure of samples and so on. Still a fairly good idea of the energy band scheme can be obtained from these observations.

Juse and Kurtschatov (11) in their investigations on electrical conductivity of Cu_2O found two values of activation energies, $\epsilon_1 = 0.7$ ev. and $\epsilon_2 = 0.13$ ev. ϵ_1 was interpreted to be the activation energy due to intrinsic conduction and to correspond to a band gap of 1.4 ev. ϵ_2 was assumed to be due to an impurity level 0.26 ev above the valence band. Engelhard (12), by measuring Hall coefficients and conductivity on samples of Cu_2O annealed in oxygen atmospheres at different pressures, deduced activation energies of 0.7 ev and 0.36 ev.

Reliable measurements of the temperature coefficient of conductivity of Cu_2O were probably first obtained by Anderson and Greenwood (13) and Böttger (14). Anderson and Greenwood observed that samples which were oxidized at 1050°C and annealed in vacuo gave activation energy of 1.04 ev and 0.30 ev, whereas samples exposed at 1020°C to oxygen at a pressure of 9 mm of Hg showed lower activation energy of 0.844 and 0.238 ev. Böttger showed that the activation is a function of oxygen at high temperatures, being 0.62 ev for oxygen pressure greater than 2×10^{-3} mm and increasing to about 0.95 ev at lower pressures. He also showed that the conductivity of Cu_2O in the pressure ranges between 10^{-2} mm. and 10 mm Hg and the temperature range between 800°C and 1000°C is proportional to 1/7th power of the oxygen pressure.

Toth et al (10) and O'Keeffe and Moore (15) have verified these results with single crystal specimens.

Results of the measurements of electrical conductivity on Cu_2O in this laboratory, by Fortin (16) and McInnis (17), show that polycrystalline samples have higher conductivity and lower activation energy than the monocrystalline samples. Experimental data indicate the existence of impurity levels lying from 0.6 ev to 1.0 ev above the valence band in polycrystalline samples and impurity levels lying from 0.6 ev to 1.0 ev above the valence band in monocrystalline samples. The band gap found is 1.8 ev to 1.9 ev.

2.2 Photoconductivity.

At any temperature, there will exist an equilibrium density of charge carriers determined by the thermal excitations and recombinations of these carriers. Therefore, if an electric field is applied to a crystal in thermal equilibrium the "dark conductivity" may be measured. Besides thermal excitations, free carriers can also be generated optically. Photons of energy higher than or equal to the band gap of the semiconductor may excite electrons from the valence to the conduction band producing pairs of electrons and holes free to move in their respective bands. These electrons and holes will produce an increment in the conductivity of the

sample over its dark conductivity and this phenomena is known as "photoconductivity." The photoconductivity produced by such band-to-band transitions is known as "intrinsic photoconductivity." If impurity levels are present in the forbidden energy gap of the semiconductor, photoconductivity will also arise due to the optical excitations of electrons to or from these levels. Photoconductivity arising due to these impurity levels is known as "extrinsic" or "impurity" photoconductivity. Since the ionisation of levels in the forbidden gap requires photons of lower energy than for band-to-band transitions, the edge of impurity absorption and consequently photoconductivity is shifted towards longer wavelength in an intrinsic photoconductor as compared to the fundamental edge which results from the band-to-band transitions.

In order to find an expression for photoconductivity in terms of the intensity of incident radiation, let us assume I_o to be the light intensity incident normal to the surface of the photoconductor. The intensity of light I after passing through a distance X of the material can be written as

$$I = I_o e^{-KX}$$

where K is known as the optical absorption coefficient. The amount of optical energy absorbed per unit time per unit

volume by the photoconductor is given by

$$-\frac{dI}{dX} = KI \qquad (2.8)$$

If $\Delta n'$ and $\Delta p'$ are the number of electrons and holes generated per unit time per unit volume due to the absorption of light in the fundamental absorption region and if $\Delta n'$ and $\Delta p'$ are assumed to be proportional to the optical energy absorbed, then we can write

$$\Delta n' = \Delta p' = \beta KI \qquad (2.9)$$

where, β the constant of proportionality, is known as quantum yield or quantum efficiency.

After a time t the density of photoexcited electrons and holes will be given by

$$\Delta n = \Delta p = \beta\, KIt \qquad (2.10)$$

The number of carriers here goes on increasing with time without limit. In order to explain steady value of photoconductivity observed experimentally we postulate a process of carrier annihilation. This process is called "recombination" and is directly related to the density of carriers present.

To find an expression for photoconductivity, we introduce the concept of "average life-time" for a free carrier. This is defined as the average time for which a carrier exists in a free state before recombining. Its value varies over a wide range (normally 10^{-2} seconds to 10^{-7} seconds) depending upon the substance and may be different for electrons and hole. In terms of average life-times, the steady state density of free electrons and holes Δn_{st} and Δp_{st} can be written as

$$\begin{aligned} \Delta n_{st} &= \beta \, KI \, \tau_n \\ \Delta p_{st} &= \beta \, KT \, \tau_p \end{aligned} \qquad (2.11)$$

and

$$\begin{aligned} \Delta\sigma_{st} &= e(\mu_n \Delta n_{st} + \mu_p \Delta p_{st}) \\ &= e\beta \, KI(\mu_n \tau_n + \mu_p \tau_p) \end{aligned} \qquad (2.12)$$

where τ_n and τ_p are electron and hole life-times,
μ_n and μ_p are electron and hole mobilities,
e is the electronic charge, and
Δp_{st} is the steady state photoconductivity.

On the basis of simple band theory, three modes of recombination are possible. These are a) direct electron-hole recombination by electron transitions to the valence

band from the conduction band; b) recombination by transitions of electrons (holes) from conduction (valence) band to impurity centres; and c) recombinations via impurity level to impurity level transitions which decreases carrier concentration upon thermal redistribution. The magnitude of the first mode is found to be negligible for pure crystals with band gap 1-2 ev. The third mode is effective only in case of large density of impurity levels. In ordinary cases we consider the second as the most influential mode of recombination.

The phenomenon of recombination of carriers through impurity levels is rather complex. For convenience impurity centres can be divided into two main categories. For one of these the energy states are very near the conduction (valence) band and are called trapping states. For the other the energy states are far away from the conduction (valence) band and are called "recombination centres or ground states." For traps the probability of return thermal transitions of carriers is very high and they can exchange carriers effectively with only one of the bands. Trapping states therefore tend to be in thermal equilibrium with their respective band edges. Recombination centres on the other hand may capture electrons and holes without return thermal transitions occurring. The lifetime of a free carrier

will be determined primarily by recombination through recombination centres. Traps will be effective only in non steady state photoconductivity specially at low temperatures.

Spectral dependence.

According to the simple band model, radiations of energy greater than the forbidden gap will produce free electrons and holes resulting in photoconductivity. But photoconductivity can arise at long wavelengths in impurity semiconductor due to electronic transition between impurity levels and bands. The magnitude of this photoconductivity is, however, small due to smaller number of states available for impurity transitions. Moss (18) has shown that it is possible to obtain activation energy from the spectral sensitivity curve of a photoconductor. He has shown that the photosensitivity for a monoatomic semiconductor falls exponentially with increasing wavelength after reaching some threshold wavelength. Optical activation energy is obtained by knowing the wavelength at which the sensitivity is one half of the maximum value. Extending the argument for excitations from impurity levels, their activation energies could also be found from the wavelength where the sensitivity has fallen to one half its value with respect to the flat part of the curve immediately preceding the exponential fall. The Moss (18) treatment, however, is valid only for non-polar crystals.

Temperature variation has a profound effect on photoconductivity but a quantitative treatment of this effect is rather difficult. In the expression for steady state photoconductivity in equation (2.12), β, K, μ, τ_p are all temperature dependent. In cuprous oxide, the dark current is greater than the photocurrent at normal temperatures. As the temperature is lowered, the dark conductivity decreases with respect to photoconductivity and the effect of trapping becomes important.

Photoconductors have generally been found to be either linear or sublinear with the intensity of radiation. Linear response occurs for low light intensity when we have a low density of optically excited carriers as compared to the density of recombination centres whereas a higher density of optically excited carriers compared with the density of recombination centres produces a sublinear response.

The DeVore effect.

If only one kind of recombination process is postulated, the spectral response curve for a photoconductor should show increasing photoconductivity with increasing absorption coefficient till a saturation value of photocurrent is reached after all the light penetrating the sample is absorbed as shown in curve a, figure 3. However, we observe

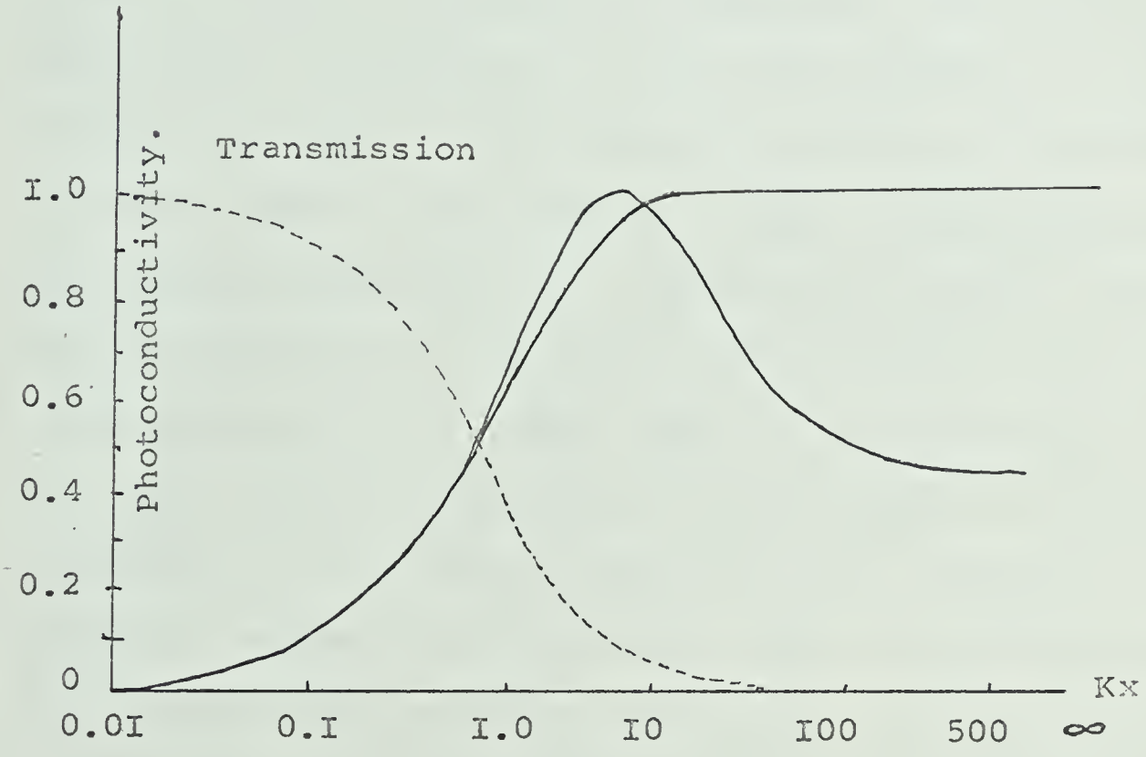

Figure 3 . Photoconductivity absorption curve.

that with increasing absorption the photocurrent rises rapidly from zero and reaches a maximum value at some moderate values of absorption. Photocurrent then starts decreasing even though the absorption is still rising and then reaches an asymptotic value greater than zero as shown in curve b of figure 3. The peak in photoconductive response curve is usually explained by asserting that due to high absorption coefficient, the light is absorbed in a comparatively thin layer on the surface producing a high density of carriers there. This leads to a high recombination rate of the carriers and hence to a reduced equilibrium concentration. This explanation is completely invalidated by the observation in substantially all cases, that the photocurrent, at least for small light intensities, is proportional to the light intensity in all spectral regions, while the peak in the spectral response curve remains. Now if the recombination of carriers were rapid due to the high density of carriers in the high absorption region, the photocurrent would have been proportional to the square root of the light intensity (sub-linear case mentioned earlier) in this region.

DeVore (19) has explained this phenomenon by assuming different recombination rates at the surface and the volume of a photoconductor. Surface recombination rate is assumed higher than the volume recombination. For such a

case the equilibrium concentration of charge carriers will be less when these are generated close to the surface than when they are generated throughout the volume. This assumption seems plausible because due to the presence of defects and absorption layers, recombination rate at the surface will be probably higher. DeVore has shown that for small values of thickness α and surface to volume recombination ratio ξ, no peak exists. For large values of α and ξ, there is a peak which becomes very rapidly more pronounced for increasing ξ and more slowly for increasing α with peak shape becoming constant for large values of α. DeVore's theory considers variation of photocurrent with Kx, where K is the absorption coefficient and x is the distance, whereas photoconductivity is usually studied as a function of wavelength. But because the absorption is related to the wavelength, we can apply the theory to the photoconductivity curves.

2.3 Excitons.

Frenkel (1) while interpreting the fundamental optical absorption spectrum in alkali halides, was first to deal with the mechanism of the absorption of light energy and its transference in a pure insulating crystal. According to Frenkel, the optical absorption in crystals could lead to

two processes: a) band-to-band transition of electrons giving rise to photoconductivity and b) excitation of the crystal lattice not associated with the appearance of electrical conductivity. In the second process the optical excitation may be transferred from the initially excited atom to its neighbour in the crystal. This mobile state of excitation was called "exciton" by Frenkel (1). Peierls (2), Wannier (3), Mott (4) and others developed these ideas a little later.

The first indications for the actual existence of excitons was obtained by the structure observed near the edge of the fundamental absorption spectra of many crystals. The structure consisted of narrow, sharp absorption lines observed towards the long wave length side of the fundamental absorption edge.

2.4 Theory of Excitons.

For most substances theory does not predict the value of the energy gap E_g between the bottom of the conduction band and the top of the valence band. Exciton levels are usually calculated with respect to the bottom of the conduction band, therefore, though all the theories of exciton predict the structure of the absorption spectrum, their position in the spectrum can be only roughly predicted.

We shall give here a brief account of the different theories with a special reference to the model applicable for our case.

The theories of excitons lean heavily on the theories of electrons in solids. For electrons in solids either one of the two basic approximations is normally applied. One utilises the Heitler-London scheme of atomic wave functions for tightly bound electrons in solids and the Hund-Mulliken-Bloch scheme for electron spread throughout the whole crystal. Any real solid lies somewhere between these limits but large classes are quite well described by one or the other. On this basis excitons have been classified into two groups:

a) Localised or Frenkel excitons,

b) Non-localised or Mott-Wannier excitons.

Localised Excitons.

Excitons found in molecular, rare gas and strongly ionic crystals are grouped under localised excitons. In this model crystals can be thought of as consisting of a collection of weakly interacting atoms (or possibly molecules). The total wavefunction for the crystal, for such a case, may be taken as the product of the electronic wave functions of its units (atoms or molecules). So if $\phi_{oR}(\underline{r})$ is the ground state wave function of the atom located at site R,

the zero order ground state is

$$\Phi_o = A\, \Phi_{oR_1}(\underline{r}_1)\Phi_{oR_2}(\underline{r}_2) \ldots \Phi_{oR_N}(\underline{r}_N) \qquad (2.13)$$

Here one valence electron has been assigned to each atom and the one electron wave functions are non-overlapping.

The excited state of the crystal may be obtained by assuming that these correspond to the excitation of a single atom into an excited state. If we assume that the atom at site R_i is in its ℓn excited state $\Phi_{\ell R_i}(r)$, the excited state can be written as

$$\Phi_\ell(\underline{R}_i) = A\, \Phi_{o\underline{R}_1}(\underline{r}_1)\Phi_{oR_2}(\underline{r}_2) - \Phi_{\ell Ri}(r_i)\Phi_{o\underline{R}_N}(\underline{r}_N) . \qquad (2.14)$$

It is clear from the translational symmetry of the crystal that the zero order energies

$$E_{ii}^{\ell\ell} = \int \Phi_\ell^*(\underline{R}_i)\, H_o\, \Phi_\ell(\underline{R}_i)\, dr_1 \ldots dr_N , \qquad (2.15)$$

are independent of $\underline{R}_i$ resulting in an N-fold degeneracy.

But each of the excited states is equivalent to, or is in resonance with, excited states localised at other points in the lattice, so the equation 2.14 is not a proper eigenstate. By the Bloch Theorem, however, linear combinations

of equation 2.14 , which are changed only by a phase factor $e^{i\underline{K}\cdot\underline{m}}$ when a primitive translation $\underline{m}$ is made on the coordinate of the system, may be proper eigenstate of the system. Thus the proper eigenstate is given by

$$\Phi_\ell(\underline{K}) = \frac{1}{\sqrt{N}} \sum_j e^{i\underline{K}\cdot\underline{R}_j} \Phi_\ell(\underline{R}_j) \qquad (2.16)$$

The new first order eigenvalues corresponding to these states are

$$\begin{aligned} E_\ell(\underline{K}) &= \int \Phi_\ell(\underline{K})\, H_o \Phi_\ell(\underline{K})\, d\underline{r}_1 \ldots d\underline{r}_N \\ &= E^\ell_{ii} + \sum_{i'} e^{i\,\underline{K}\cdot(\underline{R}'_i - \underline{R}_i)} E^\ell_{ii'} \end{aligned} \qquad (2.17)$$

The set of eigenvalues (2.17) labelled by N different wave-vectors $\underline{K}$ constitute an exciton band. E^ℓ_{ii} can be computed on the one-electron per atom model. $E^\ell_{ii'}$ is related to the probability that the excitation energy will jump between the atoms at $\underline{R}_i$ and $\underline{R}_{i'}$.

Instead of considering the excitations to be localised at a particular ion site, we can consider the volume of excitation to increase and cover several atoms. Models of this kind have been extensively examined by Dexter (24), Overhauser (25), in the case of alkali halides.

Energies of excitation for localised excitons, derived from these approaches, are approximate and we get only a qualitative picture of the overall excitation spectrum. If we apply this approach in the case of solids for which the excitons are weakly bound it is less practical. For such solids we have to utilise another approximation.

Non-localised Excitons.

In contrast to strongly ionic crystals, the attraction between constituent atom or molecules is large in covalent crystals or ionic crystals with strong covalent character. The electrons will be loosely bound to the constituent atoms or molecules and may be thought to move in the average field of all the constituent atoms or molecules with the periodicity of the lattice. In this approximation the fundamental excitation is the transfer of an electron from the valence to the conduction band leaving behind a hole. The coulomb interaction of the electron-hole pair causes the formation of a bound positronium-like state with large radius. These large radii hydrogen-like excitons, in which electron and hole move around each other and at the same time move through the crystal, are called "Mott-Wannier excitons." Instead of going into the mathematical details of the theories for such excitons, we describe below a simple model as given by Mott (4) as observed in Cu_2O.

Mott's Model.

If an electron is removed from an atom in the crystal, it may remain under the influence of the coulomb potential of the hole that remains as well as the periodic potential of the crystal lattice. With Mott, we assume that the excited electron and hole are attracted to one another under a coulomb potential given by

$$V = -\frac{e^2}{\epsilon_o r} \tag{2.18}$$

where ϵ_o = optical dielectric constant,

r = electron-hole distance.

Then, we have a simple two particle Schrödinger equation

$$-\left(\frac{\hbar^2}{2\mu}\nabla^2 + \frac{e^2}{\epsilon_o r}\right)\psi = E\psi \tag{2.19}$$

The solution of this equation gives us a set of quantised energy states which are similar to those for the hydrogen atom. The binding energy vanishes at the bottom of the conduction band. In calculation of the energy, the electron and hole masses are replaced by their effective masses m_e^* and m_h^* in the conduction and valence band and the reduced mass of the exciton is given by

$$\mu_e = \frac{m_e^* m_h^*}{m_e^* + m_h^*} \tag{2.20}$$

The energy levels are given by

$$E_b = E - E_c = - \frac{\mu_e e^4}{2\hbar^2 \epsilon n^2} \tag{2.21}$$

where n is a quantum number, and

E_c is the energy of the electron at the bottom of the conduction band.

Equation (2.21) can also be written as

$$E/hc = \frac{E_c}{hc} - \frac{R_e}{n^2} \tag{2.22}$$

where R_e is the excitonic Rydberg constant given by

$$R_e = \frac{R \mu_e}{\epsilon_o^2 m_o} \tag{2.23}$$

where R is the atomic Rydberg constant, and

m_o is the mass of a free electron.

The radius of the exciton, as calculated from the above, is given by

$$\gamma_e^n = a_o \frac{\epsilon_o m_\epsilon}{\mu_e} n^2 \tag{2.24}$$

where a_o is the radius of the first orbit of the hydrogen atom.

From the experimental value of the excitonic Rydberg constant, we can calculate the values of the radii of the exciton. The position of the exciton lines in the spectra obtained in the optical absorption of Cu_2O at low temperature shows a surprisingly good agreement with formula (2.22) for $n > 2$. The above simple model is only valid for excitonic spectra in isotropic crystals.

Thus, according to the exciton model, we should expect, over and above the main absorption band due to band-to-band transition of electron, a series of absorption lines corresponding to the transition of electron from the valence band to the exciton levels near the conduction band in the forbidden gap. The wave number of these lines is given by equation (2.22).

The transitions of electrons from the valence band to the exciton levels must follow certain selection rules. According to Elliott (20) two classes of transitions are possible and the excitons are labelled accordingly. The spectra of the first class results from direct transition in which $\Delta\underline{K} = 0$ and wave vector $\underline{K} = 0$ i.e. no change occurs in the initial and final wave vector of the electron. In this class, only transition to "s" exciton states are allowed. The spectrum then consists of hydrogenic series lines corresponding

to the principal quantum number $n = 1,2,3 \ldots$ The oscillator strengths (ratio of the quantum theoretical and classical contributions of transition from state m → state p to the refractivity N-1, where N is refractive index) of the lines in the series are of the order $(n\epsilon)^{-3}$. The second class of spectra belong to the forbidden transitions in which $\Delta\underline{K} = 0$ but the wave vector K has a small value. In this class of spectra the only transitions allowed are to p-exciton states. The spectrum will consist of a hydrogenic series of the line in which the first term will be corresponding to n = 2. The intensity of this class of spectra is much smaller than the first class. The oscillator strength of the first line is $\approx 0.03\epsilon_o^{-5}$ and those of the succeeding lines vary as $(n^2-1)n^{-5}$. The spectrum of Cu_2O according to Nikitine (21) belongs to the second class of spectra as described by Elliot.

2.4 Optical Exciton Spectra.

Survey of literature:

Optical absorption spectra of Cu_2O have been thoroughly investigated by many research workers belonging to the Russian group (Gross), the French group (Nikitine) and in Japan by Hayashi.

The absorption spectra of Cu_2O consists of two absorption edges in the red region of spectrum about 208 cm^{-1} apart. At high temperatures, these two edges do not remain distinct, because another strong absorption edge is partly superimposed on the two red edges at these temperatures. The absorption spectra of Cu_2O in the red region is shown in figure 4. At low temperatures, however, the absorption edge superimposed upon the two red edges vanishes and instead, one gets two sets of structure consisting of sharp, narrow, hydrogenic-spectra-like lines, situated at the high energy side of the red edges. These two sets of lines are in the yellow and the green regions of spectrum and have been discovered independently by Hayashi and Katzuki (22), Nikitine et al (23) and Gross and Karryev (5). One absorption continuum is observed between the yellow and the green series and another continuum at the series limit of the green series. On the short wavelength side of the green series one can observe two strong absorption peaks in the blue and violet regions.

The wave number of the yellow and the green series at 77°K can be expressed by the formulae:

$$\text{yellow series:} \quad \nu_n = \nu_\infty - \frac{R_e}{n^2} = 17459 - \frac{795}{n^2} \ cm^{-1}, \quad n = 2,3,4...\infty \tag{2.25}$$

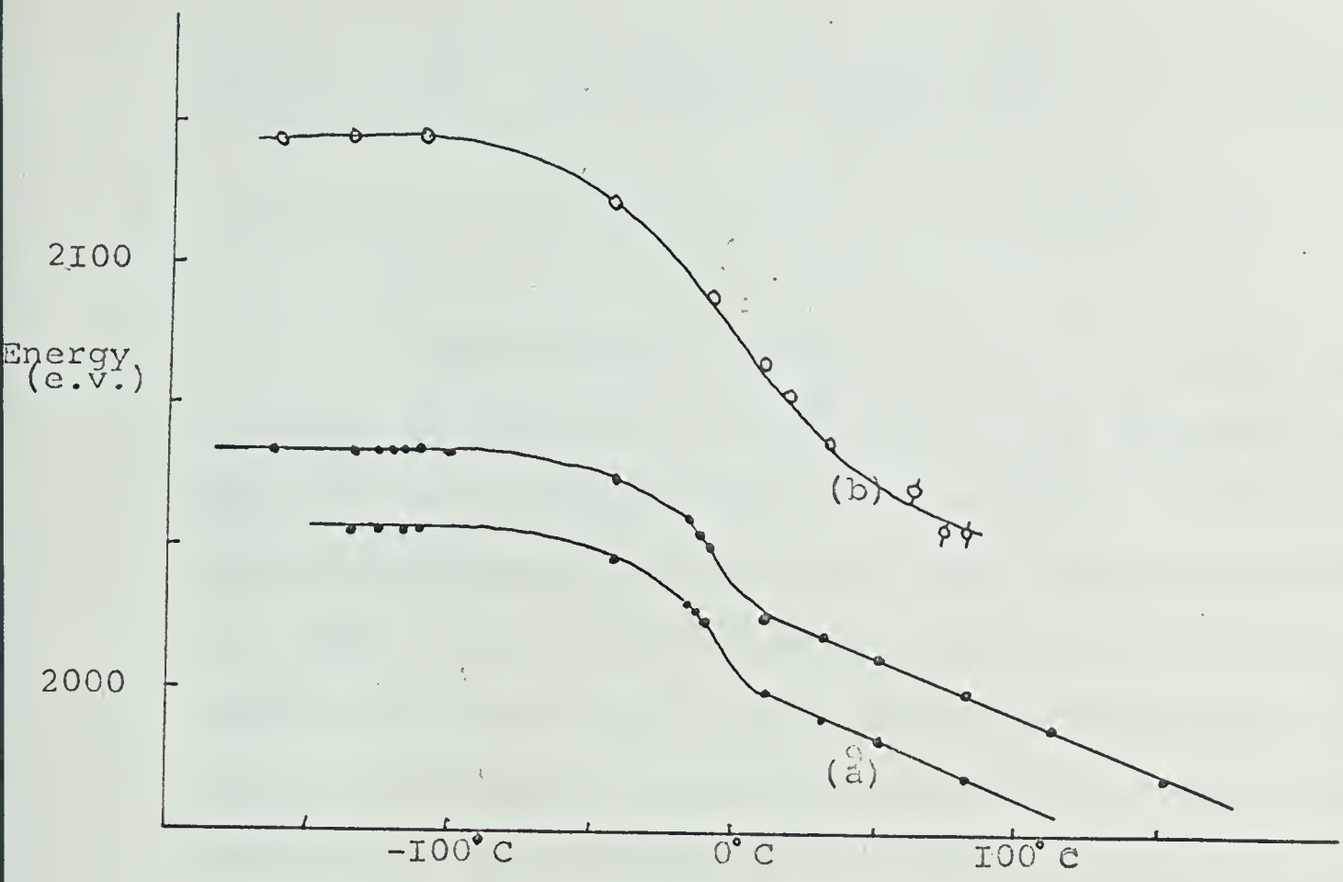

Figure.5. Variation of red absorption edge with temperature

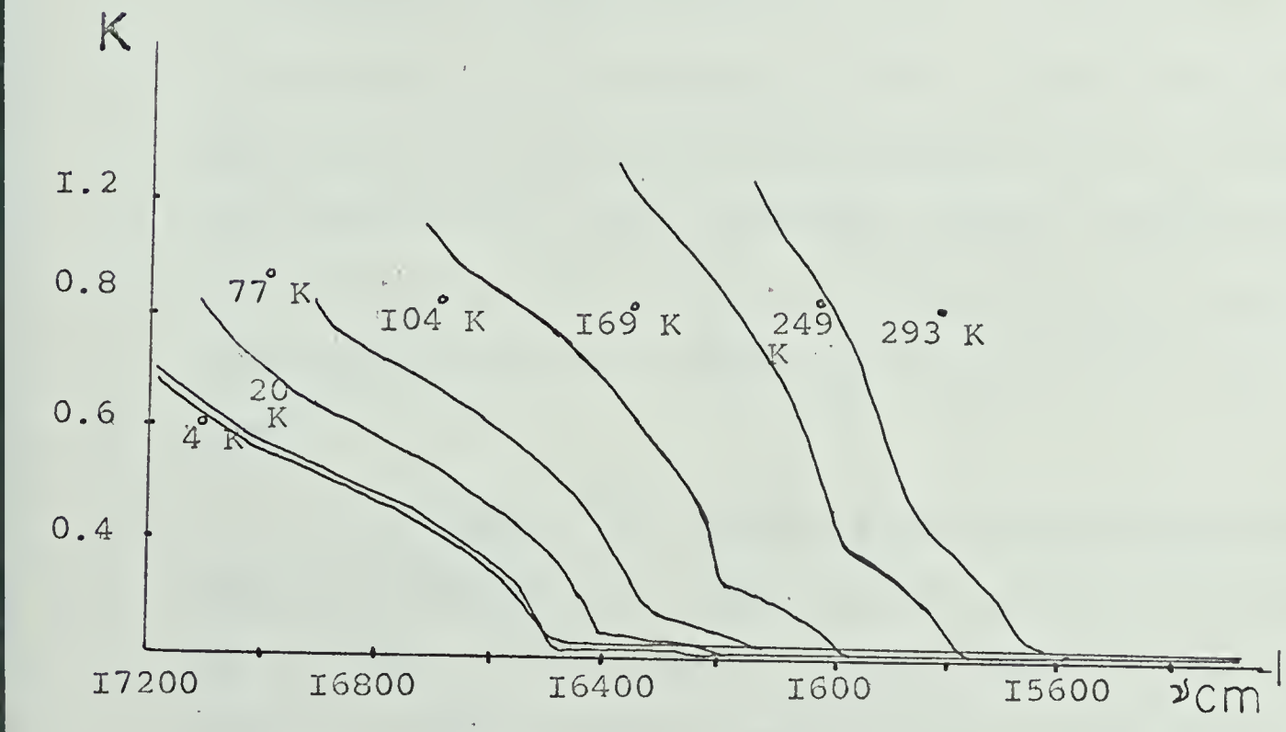

Figure.4. Absorption curve of Cu_2O at various temperatures.

green series: $\nu_n = 18514 - \frac{1252}{n^2}$ cm^{-1} , n = 2,3,4...

(2.26)

For the yellow series line for n = 1 has also been observed at 6095.8 A^{o} at 4.2^{o}K but it is displaced by 340 cm^{-1} as calculated from the hydrogenic formula. As for such discrepancy Gross and Haken (33) have discussed that the orbit for n = 1 is so small that the interaction potential between the electron and hole is not expressed by $-\frac{e^2}{\epsilon_o r^2}$. Gross and Hayashi considered that green and yellow series arise due to the transition of electrons from the common ground state to the two series of energy levels which converge to different ionisation states, i.e., two sets of levels converging at the conduction band. If one scrutinises the spectrum obtained by Gross and Karryev (5), it is concluded that the absorption coefficient decreases towards shorter wavelength side from the series limit of the yellow series and reaches a minimum at 5500 A^{o} suggesting a structure in the conduction band.

Hayashi (26) obtained two sharp edges and a weak edge in the absorption spectrum of Cu_2O in red region shown as a and b in figure 5. He has observed that both the edges a and b shift towards longer wavelength with the

rise of temperature but that the energy difference between two absorption edges a remains constant. He also found the shift of absorption edges to be a linear function of temperature at higher temperature ($0^{o}C$ to $150^{o}C$) but shows an entirely different behaviour at lower temperatures as shown in the left hand portion of figure 5. Nikitine (27) has shown that the square of the absorption coefficient is a linear function of frequency at different temperatures. If K_1 and K_2 be the absorption coefficients in the two red continuum and ν_1' and ν_2' be the frequency of the two edges, then the experimental values of absorption coefficients are represented very accurately by a relation

$$K_1 = a_1(\nu' - \nu_1')^{1/2} \quad \text{and} \quad K_2 = a_2(\nu' - \nu_2')^{1/2}$$

where a_1 and a_2 are strongly temperature dependent and the experimental results are accurately represented by

$$p_1 = \frac{K_1}{(\nu' - \nu_1')^{1/2}} = \begin{cases} C_1 T & \text{for large values of temperature } T \\ 0 & \text{for } T \to 0 \end{cases}$$

$$p_2 = \frac{K_2}{(\nu' - \nu_2')^{1/2}} = \begin{cases} C_2 T + C_3 & \text{for large values of temperature } T \\ C_3 & \text{for } T \to 0 \end{cases}$$

In the yellow region the Strasbourg group has observed up to five lines whereas Gross has observed as many as nine lines which is exceptional. Hayashi (26) on the other hand could see only three lines and one absorption edge in this region. He observed that the lines and the absorption edge in the yellow region undergo the same shift with the variation in temperature and the energy difference between them always remains constant. The oscillator strength of the line corresponding to $n = 2$ and $n = 3$ are $2.8 \times 10^{-6} \pm 6\%$ and $1.0 \times 10^{-6} \pm 10\%$ and their relative intensities lies between 1/2.6 and 1/2.9. The absorption coefficient for yellow continuum seems to obey the theoretical formula $K \propto (\nu - \nu_\infty^{y})^{3/2}$ for $\nu \gg \nu_\infty^{y}$ as is shown by the Strasbourg group (28).

In the green region the absorption lines obtained are broad. Hayashi (26) observed four lines at $-180^{\circ}C$ and their number decreases at higher temperatures. The two lines counted from longer wave length side are broader in width than the others. Hayashi observed that the variation of the energy difference between the lines appearing at the long wave length side of the yellow and green series remained constant below $-70^{\circ}C$. The oscillator strength of only the first line has been calculated and is given as $2.8 \times 10^{-5} \pm 10\%$. For $n \geq 3$, $K \propto 1/n^2$ and the breadth of line decreases with increasing n (quantum number).

The spectrum of cuprous oxide undergoes changes by a) electric fields, b) magnetic fields, c) strains, d) neutron and γ-ray irradiation, etc. The electric field produces the splitting of lines in different components, shifting of series to longer wavelength, reduction of intensity etc. These and other effects become more pronounced with increasing field intensity. The so-called Zeeman splitting of the exciton lines is observed by the application of the magnetic field. Strains in general cause the shifting of the lines.

2.5
Photoconductivity at Exciton Wavelengths

Since excitons are electrically neutral pairs of electrons and holes, they cannot carry current. In real crystals, however, one usually does observe photoconduction as a result of optical absorption in the exciton band. To explain this we have to consider the fate of an exciton after it is formed. Different cases may arise: a) once created, the exciton can be annihilated either by emitting same radiation or without radiation, b) the exciton may dissociate at an impurity or defect and the majority carrier (hole in our case) can be trapped. The minority carrier left can immediately recombine with a majority carrier. c) The exciton may dissociate with the liberation of a majority and a minority carrier which may have a reasonable lifetime. d) The exciton may dissociate and the minority carrier may be trapped. In cases a) and b) no photocurrent can be expected when light is absorbed in an exciton line. For cases c) and particularly d) photocurrent may be expected when the crystal is irradiated in the line.

In any case the exciton must dissociate and therefore we briefly look into the causes of dissociation of excitons. The excitons may dissociate by the following mechanisms: (i) dissociation by phonons; (ii) collision ionisation; (iii) dissociation by or ionisation of static imperfections.

(i) Dissociation by phonons:

In pure crystals, phonons are the principal perturbations required for the breakup of an exciton. In this process phonons and the kinetic energy of excitons must supply the energy needed for the dissociation which is

$$\frac{R_e}{n^2} + \Delta E$$

where R_e = excitonic Rydberg constant

ΔE = the energy in excess of the energy band gap.

The only quantitative work on this mechanism seems to have been done by Lipnik (31) and Goodman and Oen (32). Lipnik obtains the following expression for lifetime against dissociation by single-phonon-process for a non-polar Wannier model exciton

$$\tau_d = \frac{(2\pi h^2)^{3/2}}{3^{1/2}\mu_e (KT)^2} \cdot \frac{1}{\sigma_{ph}} e^{\Delta/KT}$$

where,

μ_e = exciton reduced mass,

$\Delta = R_e/n^2$, binding energy of the exciton,

σ_{ph} = cross section for phonon-induced decay of exciton being independent of temperature.

In Cu_2O, the lifetime of a thermal 1s exciton computed from the above equation by putting $\Delta E = 0.15$ ev is given by

$$\tau_d = 6 \times 10^{-12} \text{ seconds at room temperature}$$
$$= 6 \times 10^{-6} \text{ seconds at } 100^{\circ}K.$$

The cross section σ_{ph} is found to be of the order of 10^{-13} cm^2 in Cu_2O.

Phonon decomposition of excitons will be more probable in cases where exciton bands are narrow and intense and converge very closely to the continuous absorption edge. This is the case in Cu_2O, BaO, CdS, etc. In alkali halides where the difference between exciton levels and the ionisation continuum is large, this process is less probable.

(ii) Collision Ionisation:

At high exciton density two excitons may collide to produce the pairs of free electrons and holes. Choi and Rice (34) have shown that the transition rate from the former to latter for Frenkel model can be given by

$$\frac{dn}{dt} \approx - \left(\frac{n^2}{Na^6}\right) \times 10^{17} \text{ sec}^{-1}$$

in a tetragonal crystal in which $c >> a$ (a and c are unit cell dimensions), where n is the density of randomly distributed excitons and N is the number of unit cells in crystals.

The dependence of dissociation rate on n^2 means that a similar dependence on light source producing excitons should exist. The experimental verification of this process by Apker and Taft (35) on RbI for photoelectric emission could not verify this even when the light intensity was increased ten times. Choi and Rice (34) pointed out, however, that this effect will be difficult to verify experimentally due to the generation of carriers at the surface. Moreover, when electron-hole recombination probabilities are high, the observed photocurrent becomes linear with light intensity.

(iii) Dissociation by or Ionisation of Static Imperfection:

This is probably the most probable mode of the production of free carriers by excitons. A static imperfection or impurity cannot readily dissociate an exciton whose energy level lies below all conducting states because the energy will not be conserved. In order to overcome the binding energy of exciton for dissociation of excitons, the exciton kinetic energy will have to be employed. But an exciton produced by photoexcitation has very little kinetic energy. In order to suffer an inelastic dissociation exciton must encounter an excited defect. The excited defect will transfer its excitation energy to the exciton thereby causing its dissociation. Lipnik (31) has considered the case of dissociation of excitons with neutral impurities and concludes that phonon dissociation will be dominant mechanism.

The excitons on the other hand might ionise the imperfections in the crystal. Here the exciton might disappear transferring its entire excitation energy to the freed electron or hole. This mode was utilised by Apker and Taft (35) to explain the spectral photoemissive response in evaporated films containing large number of F centres (negative ion vacancies which trap electrons). They concluded that energy is being transferred from excitons to the F centres. Phillip and Taft (36) calculated the cross-section for exciton induced ionisation as less than 10^{-14} cm^2. We can visualise the ionisation of acceptors and donors in the similar way.

Survey of literature:

Exciton induced photoconductivity has been a matter of investigation by many research workers such as Gross & Pastrnyak (8), Apfel and Portis (9), Coret and Nikitine (37), Pastrnyak and Timov (38) and many others. The result of these workers vary over a wide range due to variations in many parameters on which the photoconductivity depends. The theory of photoconductivity in connection with excitons has not been worked out and the experimental results can only be explained in a qualitative or semiquantitative way with whatever theoretical explanations we have. We shall present here the pertinent observations of different workers with their possible explanations.

Gross and Pastrnyak (8) were first to find the correlation between the optical absorption due to excitons and the corresponding structure in photoconductivity curve for Cu_2O. Their observations were made on the natural surface of single crystals and polycrystals of Cu_2O 300 to 400 microns thick at the liquid nitrogen temperature and with light chopped at 8 cycles/second. Superimposed upon the background photocurrent, they found a peak of photocurrent at $\lambda = 6124$ A^o. This corresponded to the absorption line at 6125 A^o corresponding to the $n = 1$ transition in the yellow exciton series.

The photopeaks observed at λ = 5792 A°, 5752 A° and 5740 A° corresponds exactly to the absorption lines for n = 2, 3, and 4 in the yellow exciton series. In the green region of spectrum three peaks were observed at λ = 5487 A°, 5433 A° and 5414 A° which agreed within limits of accuracy to the wavelengths measured for n = 2,3, and 4 in the green exciton series. Since the magnitude of the stationary photocurrent depends upon the amount of light absorbed in the crystal, the quantum efficiency, and the lifetime of the carriers, they concluded from observing the peaks in the exciton absorption lines that there is a new photoconducting mechanism which involves either a change in lifetime of the carriers or a change in quantum efficiency.

Apfel and Portis (9) also observed structure in the photoconductivity spectrum of Cu_2O. Using modulated light at 4 cps they observed peaks superimposed on the background photoconductivity in the yellow region of spectrum at 35°K and 170°K in a low resistance multicrystalline sample of Cu_2O. With continuous illumination at 100°K they observed structure in the vicinity of the green series but the lines appeared to be inverted. The positions of minima in the photoconductivity coincided with the positions of the absorption lines in the yellow exciton series. In this case the position of these minima were found to be slightly

dependent on the rate at which the incident photon energy was varied. This suggested a relaxation time in photoconductivity which was found to be of the order of tens of seconds. To account for the difference in a·c conductivity and steady conductivity they reasoned that there must be an initial rise in photoconductivity when the light is turned on followed by a decay of exciton associated conductivity to a negative value. By shifting photon energy rapidly from a position just off the line onto it, they observed a rapid rise in the photoconductivity of the sample followed by a decay to below the initial value, suggesting some sort of relaxation mechanism. To explain the production of free carriers by excitons, they postulated two mechanisms: 1) ejection of carriers from states in the gap, 2) the dissociation of excitons by phonons. Due to the slight temperature dependence of the exciton induced photoconductivity they ruled out the second probability. The excitation of localised charges by excitons seemed the most probable.

Pastrnyak and Timov (38) also observed photoconductivity peaks in the green and yellow exciton series in single crystals of Cu_2O of thickness 0.3 to 1 mm using a chopped light at 8 cps. At liquid air temperature they also obtained two maxima of photoconductivity at 4850 and 4610 A^{o} which coincided with the maximum observed in the reflection curve of the same samples and corresponded to exciton

absorption in blue and violet region. They also observed negative photoeffect when the voltage across the sample was increased (E = 2 kv/cm) in the spectral region extending up to 4850 A^{o} on the short wave length side. This negative effect increased with increasing voltage across the specimen. In the region where it was observed increase in voltage (e.g. at 5240 A^{o} an increase from 1 kv/cm to 3 kv/cm) was sufficient to make a transition from a positive to an entirely negative photoeffect.

To explain the mechanism of the generation of carriers in the exciton lines they postulated the dissociation of excitons by lattice vibrations (phonons) on the basis of the photoeffect from the line with quantum number n = 2 being less than that from the line n = 3, even though their absorption was the same.

Coret and Nikitine (37) also obtained maxima and minima of photoconductivity in the exciton lines. Their observations were taken on 100μ to 400μ thick crystals of Cu_2O prepared at high temperature under "reduced oxygen pressure." The dark resistivity of the samples at liquid nitrogen temperature was 0.3×10^{9} Ω cm. For weak fields (200 volts/cm) they observed all edges in conductivity corresponding to the absorption edges in reflection and absorption spectra of the samples. They could only observe

the first lines for each exciton series which appeared as maxima of photoconductivity. The peaks corresponding to violet and blue lines were particularly intense. After the samples had been heated for 24 hours at 150°C in air, the photoconductivity spectrum in the short wave length region was disturbed. The photoconductivity peaks in blue and violet region were changed to minima of photoconductivity. The photoconductive spectrum in other regions remained unchanged. However, when left for a few days the photoconductivity regained its original form. However, profound changes in the photoconductivity were observed by increasing the applied electric field. Figure 6 shows the response curves of the sample in high electric field when it is illuminated by short wavelength ($\lambda < 5000$ A°) light and then with long wave length ($\lambda = 5600$ A°) light. For illumination by radiations of $\lambda < 5000$ A° the photocurrent increased rapidly over the dark current and then slowly attained a steady value. On the interruption of light the photocurrent did not come to the preillumination value but decreases slowly. For radiation of wavelength $\lambda = 5600$ A° however, the photocurrent in the sample increased rather sharply upon illumination at first but started decreasing later and attained a steady state value which was less than the initial dark current. This is the negative photoelectric phenomenon

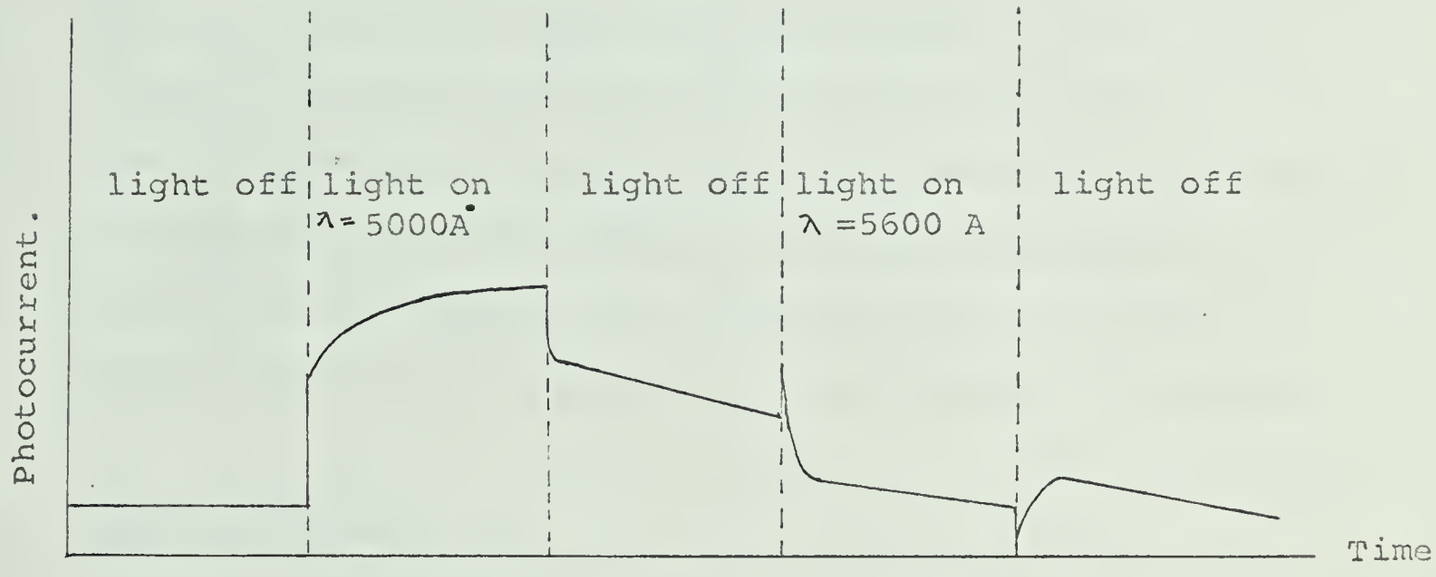

Figure 6. Photoresponse at high electric fields.

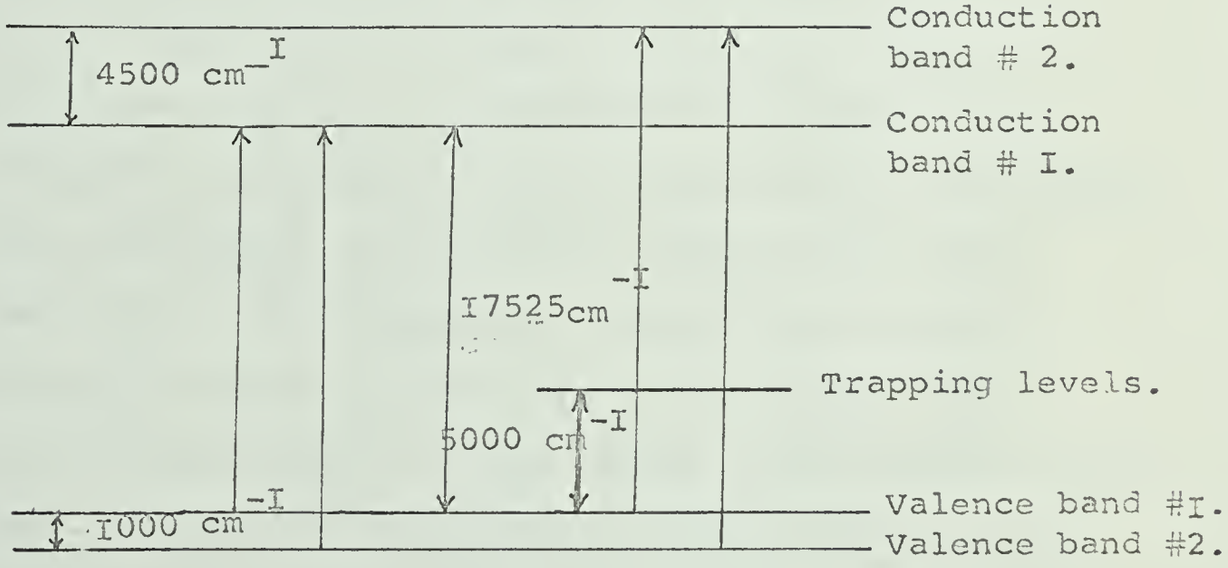

Figure 7. Energy level diagram of Cu_2O as proposed ny Coret and Nikitine.

which had previously been observed by Pastrnyak and Timov and mentioned earlier. Coret and Nikitine observed that the grain boundaries in the crystals contributed to this effect. They also observed important modifications in the photoconductivity spectrum between the wavelengths 6200 A^{o} and 5000 A^{o} for samples previously illuminated for a few minutes. The green exciton lines appear as maxima whatever be the field but the yellow series coincided with the minima of photoconductivity. The edges in red were also inversed.

Surface effects:

The condition of the surface of a photoconductor has a profound effect on the spectral curve of photoconductivity. It has been reported by many investigators that an antibarrier layer with increased conductivity exists on the natural surface of Cu_2O. Absorption of oxygen on the surface increases the concentration of carriers in the surface layer, and consequently, the surface conductivity. Thus unless the samples are homogeneous, conductivity at low temperatures will be dominated by surface effects. The absorption of polar molecules (e.g. water, ethyl alcohol, etc.), etching and polishing of the surface, on the contrary, leads to dimunition of the surface conductivity and the formation of a barrier layer. Surface polishing and, apparently,

etching also increases the concentration of defects near the surface. The surface properties can influence the photoeffect in various ways. First of all, the presence of surface fields can facilitate or hinder the diffusion of carriers towards the surface and influence the surface recombination which is analogous to increased concentration of defects near the surface. The structure in photoconductivity can be distorted by surface fields and the lack of periodicity will cause a blurring and broadening of maxima. The appearance of maxima, corresponding to the transitions to the surface levels, can also be expected in the photoconduction curves as observed by Pastrnyak and Timov (38). Therefore in order to study the relation between the magnitude of the absorption coefficient and photoconductivity it is necessary to work with specimens with a small number of defects near the surface, a minimal warping of the zones at the surface, and a small penetration depth of this warping in the crystal. Specimens with natural surfaces best satisfy these requirements. Gross and Pastrnyak (8) have studied the effect of different surface treatments on the photoconductivity spectrum of Cu_2O. They observed the following: for treated surfaces, the structure of the spectral distribution of the photoconductivity in the region of the yellow exciton series, shows the peaks of photoconductivity to be shifted and neither the peaks nor the dips to coincide with

the position exciton absorption lines. Surface polishing also leads to the blurring of the structure, specially for higher members of the yellow series. In green series this distorts the detailed structure in the photoconductivity curve even more. Heating the sample to 100°C - 150°C in air or in vacuum results in decrease of photocurrent due to increased recombination caused by the elimination of absorbed oxygen. The absorption of oxygen on the other hand leads to an increase in photocurrent.

In order to explain their observation, Coret and Nikitine (37) have given two likely mechanisms to explain these effects:

1. Passive effects

a) The exciton, once formed, can dissociate itself on a centre which provides it with the necessary ionisation energy. The dissociation provides a free electron and a hole and we observe a peak in the photoconductivity. This they call the positive passive effect.

b) The exciton, once formed, can destroy itself on a centre with the emission of a photon or giving its energy to the centre. No charge carriers are produced due to the direct recombination of hole and electron. We get a decrease in the photocurrent as part of the incident photon energy

is utilised in creating excitons which do not contribute to the current. This process is called the negative passive effect.

2. Active effect

Coret and Nikitine have suggested another probable mechanism to explain their results of photoconductivity in exciton lines:

c) The exciton after it is formed, may dissociate on a centre which traps the hole.

d) The exciton after it is formed, may dissociate on a centre which traps the electrons.

If the holes are trapped after the dissociation of the excitons, as suggested in c), the residual electrons may recombine with the holes. This will result in the diminution of holes, which are majority carriers in Cu_2O and a subsequent decrement in the photoconductivity due to excitons. On the other hand, if the electron is trapped, the residual hole will increase the number of majority carriers in the crystal and an increase in photoconductivity at exciton wavelengths may result. The negative photoeffect has been interpreted by them as due to the presence of hole traps on the

surface, and electron traps on the boundary between the grains when heated to 150°C. They have given a tentative band scheme for Cu_2O as shown in Figure 7 to explain the phenomena of photoconducting. The band scheme is due to Elliot (39) except that trapping level has been added at 0.6 ev above the higher valence band.

CHAPTER III

EXPERIMENTAL PROCEDURE

3.1 General requirements

In order to prepare high resistivity crystals of Cu_2O extreme care has to be taken to avoid all forms of impurities in the crystals. Copper, for preparing the samples, should be of utmost purity and care should be taken that no impurity contaminates the sample during and after its preparation. For photoconductivity measurements the samples should be of such a thickness that all the incident light, in the region of interest, should be completely absorbed in it. The electrical contacts to the sample should be non-rectifying and of low resistance. To minimize the noise, the sample should be rigidly fixed. Due to high resistance of Cu_2O crystals, stray capacitance and electrical pickups pose a serious problem. High input impedence measuring instruments have therefore to be used and the distributed capacitance should be kept as low as possible. The different electrical connections as well as the sample should be electrically shielded. The samples should also be optically shielded for photoconductivity measurements.

The sample holder should be so constructed that it should withstand large variations of temperature (from liquid nitrogen temperature to 950°C) and should maintain high vacuum at all temperatures. Maintainance of high vacuum is very important in the case of Cu_2O. This is because oxygen, as a stoichiometric excess in Cu_2O, acts as an impurity. The sample holder should also provide a good thermal contact with the surroundings. The light source to be used should be such that the distribution of spectral intensity should not change for different observations. For this we have to choose such a source which does not deteriorate easily and the electrical current feeding the light source should be held constant The monochromator should provide an output of high spectral purity and should have a high resolution because exciton lines, especially in yellow series do not have large wavelength differences.

3.2 Procedure

a) Preparation of sample.

The Cu_2O samples, used in these experiments, were grown from 99.999% pure copper obtained from American Smelting and Refining Company, using the technique described by Toth et al (10). After oxidation and annealing, the samples were allowed to cool in vacuo (10^{-4} mm of Hg) for a

period of about 24 hours. The method of preparation of the samples has been dealt with in detail by Fortin (16). The crystals obtained were in the form of slabs varying in thickness from 0.3 mm to 0.5 mm. The crystals of 2.5 cm x 1.0 cm size were cut such that the region of interest consisted of a single crystal. Two electrodes, for electrical contact to the sample, were applied by sputtering a thin layer of platinum on the sample in an argon atmosphere. A gap of 0.5 mm was left between the electrodes for optical investigations. Electrical contacts to the platinum electrodes were made by wrapping bands of platinum around the electrode. To these bands were spot welded a chromel wire on one side and a Chromel-Alumel thermocouple at the other side which served as an electrical contact as well as a thermocouple for measuring temperature.

b) Sample holder.

The vacuum jacket surrounding the sample holder consisted of a demountable vacuum seal which works on a surface friction effect instead of compression and is described by Brymner and Steckelmacher (30). It consisted of two stainless steel flanges with a male cone on one flange and a mating female cone on the other flange. A gasket of thin copper (.01 in.) was placed between the surfaces of the male

and female cones of the flanges and was bolted by means of screws fitted in the flanges to produce a leak tight seal. No leakage was observed with this device up to a temperature of 950°C. The glass part of the vacuum system was sealed to the male flange which was mounted rigidly to a stand. A quartz tube 3.8 cm in diameter and 15 cm long was sealed to a Kovar tube of the approximately same diameter by means of a quartz-pyrex and a pyrex-Kovar seal. The Kovar in turn was then silver soldered to the detachable female flange. A plane quartz window was sealed in the quartz tube in front of the sample for the passage of light. The sample and the electrical leads were supported from the fixed flange by stainless steel rods and with steatite insulators which had been fired at high temperatures in hydrogen atmosphere. This set-up could easily withstand the maximum temperature required in the experiments and the electrical insulation between the leads exceeded 10^{14} ohms. A vacuum of the order of 10^{-7} mm of Hg was routinely obtained. The sample holder is shown in figure 8. The sample was cooled by surrounding the vacuum jacket by a dewar flask which was filled with liquid nitrogen. Thin copper sheets were wrapped around the dewar and aluminum foil were wrapped on top of the dewar serving the two-fold purpose of avoiding electrical pickup and shielding against stray light falling on the sample. The

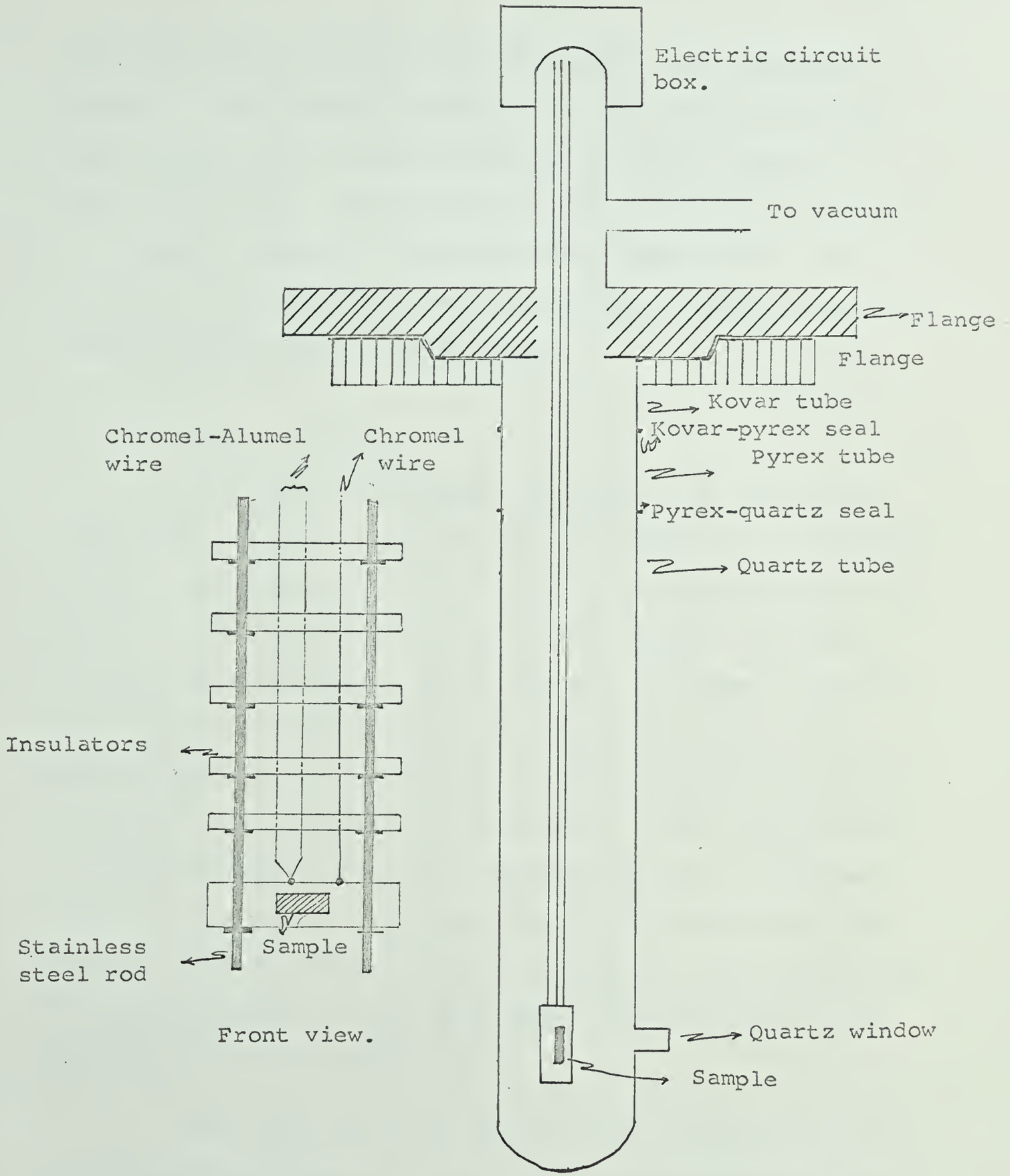

Figure 8. Sample holder.

dewar was unsilvered at the place in line with the quartz window to allow for the passage of light. Surrounding the holder simply with liquid nitrogen, cooled the sample to about 123°K only. Pure helium gas was leaked into the system to bring the sample to liquid nitrogen temperature. The temperature of the sample was read by measuring the e.m.f. of the thermocouple by a potentiometer.

c) Optical equipment.

The optical equipment consisted of a flint glass prism Kipp and Zonen mirror double monochromator (L 3544-5210) having a maximum resolution of 15 A° in the visible region at the slit width used (0.1 mm for all the slits). The monochromator was calibrated before using in accordance with the manufacturer's instructions. The green line 5461 A° of mercury obtained from a mercury discharge lamp was taken as standard for the purpose of calibration. After calibration at this wavelength, the other wavelengths were in agreement with the calibration curve supplied by the manufacturer and any arbitrary wavelength could be determined from the reading of the wavelength drum and wavelength corresponding to this reading in the calibration curve.

The light from the monochromator could be focussed on the sample by means of a pair of front aluminized mirrors. The output slit, the mirrors and part of the sample holder

were enclosed in a light tight aluminum box to avoid electrical and stray light pick up. The wavelength drum of the monochromator could be changed continuously either by hand or by two electrically driven motors of different speeds provided internally or by an external synchronous electric motor of variable speed. A contact disc sent electrical signals for every 5 minutes of rotation of the wavelength drum and was used to drive an indicator pen in the recorder.

A tungsten ribbon filament G.E. lamp 18 A/T 10/1P-SR8 was used as the source of light for photoconductivity measurements. A current of 18 amperes at 6 volts was supplied by a Lambda constant current power supply model(LE 104 FM). The lamp had advantages over other gas filled filament lamps in that: a) the filament deterioration due to evaporation etc. was small; b) higher light intensity in shorter region; c) greater intensity of light for shorter wavelengths due to higher filament temperature.

d) Electrical circuit.

The electrical set-up for measuring d.c. photocurrent was of a standard type and is shown in figure 9. The change in photocurrent was measured across a resistance connected in series with the sample. This resistance adjusted in magnitude depending upon the resistance of

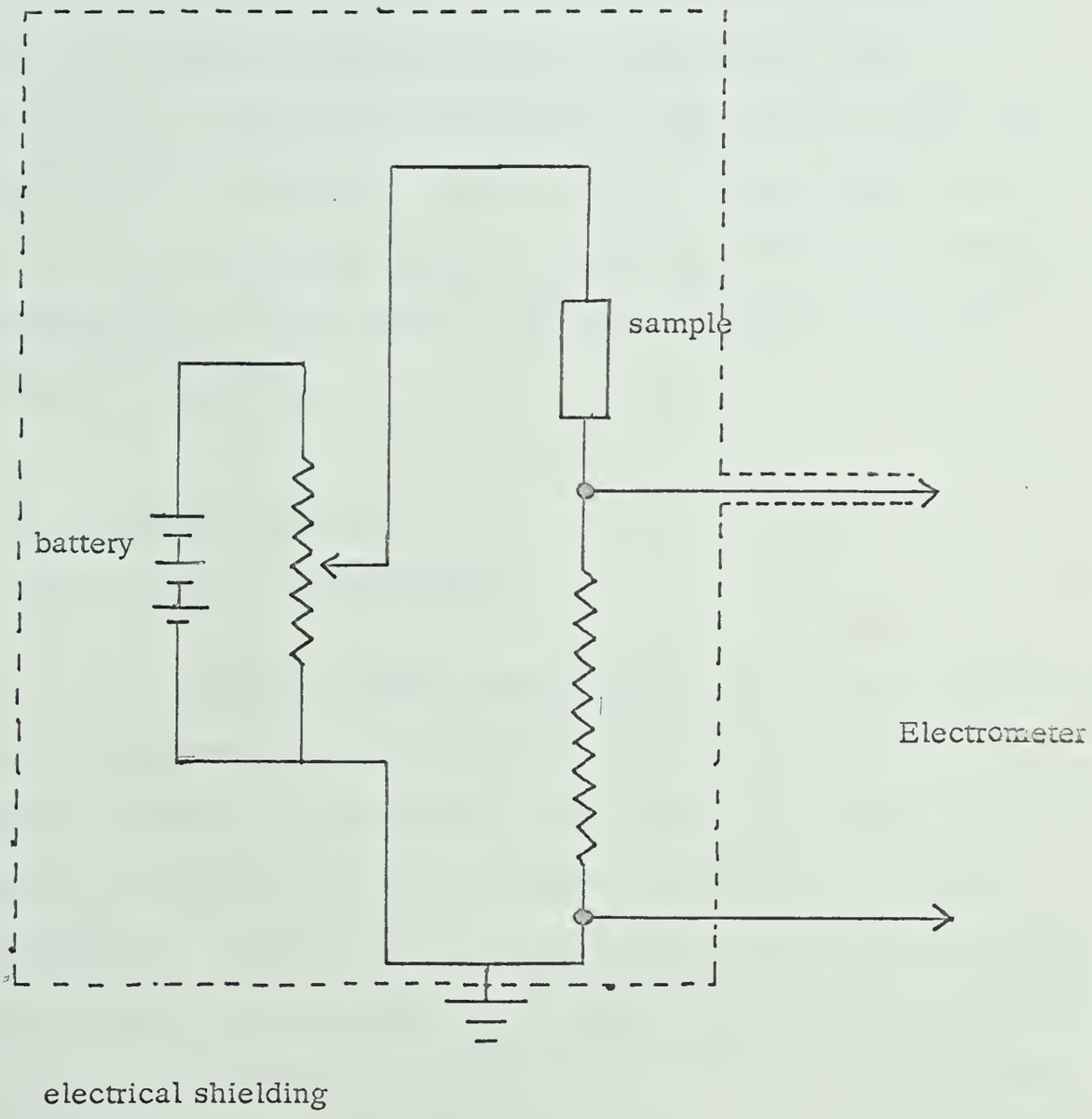

Figure 9. Schematic diagram of the electrical circuit.

the sample and the strength of the signal desired. A set of dry batteries in series and a potentiometric arrangement was used to apply variable potentials across the sample. The potential drop across the resistance was measured by means of a Carey vibrating reed electrometer model 31 V. The output of the electrometer was then fed to a Westronic model S11 A/U recorder. Due to the very high impedence of the circuit, the whole system including batteries, sample and connecting cables were very well shielded to avoid electrical pick up.

3.3 Procedural details

a) R vs $\frac{1}{T}$ measurement.

Before taking observations for photoconductivity, a set of observations were taken for resistivity of the samples. These observations were taken for freshly installed samples as well as for the samples heated at different temperatures. Observations were taken both during heating and cooling of the samples. At high temperatures an avometer was used for resistance measurement whereas, at low temperatures, a Radiometer Copenhagen megohmeter capable of measuring resistances in the range of 10^{14} ohms, was used.

b) Photoconductivity.

Measurements on photoconductivity were made on single crystals of Cu_2O. Pure helium gas was leaked into the system to bring the samples at liquid nitrogen temperature. Structures observed in photoresponse curves were fairly reproducible. Observations presented here were taken with a crystal whose photoresponse was first taken with the natural surface. It was then heated to 150°C in vacuum and the photo-response taken. Photoresponse was also taken by etching the surface of the crystal by dilute nitric acid, followed by heating this sample at 150°C and 950°C in vacuum. Finally the sample was heated in air and the photoresponse was again measured. Variable voltages (2 Kv/cm, 1 Kv/cm, 40 volts/cm) were applied for each set of observations. The dispersion of the monochromater was not linear, therefore the recorder chart readings had to be replotted for better interpretation of the observations. As we were only concerned with the relative observations, the response curves were not plotted for constant intensity throughout the spectral region and therefore the slopes of the exciton peaks are insignificant.

CHAPTER IV

RESULTS AND DISCUSSION

4.1 Electrical conductivity.

Electrical conductivity measurements were carried out to investigate the characteristics of the samples and to provide a comparison with similar results of other investigators.

The observations on conductivity were taken under high vacuum conditions (10^{-6} to 10^{-7} mm of Hg). These observations were obtained both for unheated samples and samples outgassed at different temperatures. The outgassing was usually done at about 150°C, 250°C, and 950°C. The outgassing time at 150°C varied from several hours to a day. Except for two samples, we had very little success in outgassing the samples at temperatures higher than 390°C. The samples near this temperature had a strong tendency to reduce forming a thin layer of copper on the surface of the sample in a matter of seconds. The two samples not reduced, were heated under a relatively poor vacuum ($\sim 10^{-4}$ mm of Hg) obtained by a mechanical pump. All the other samples heated when the mercury diffusion pump was on in the system invariably reduced. Pressure seemed to have an effect on this phenomenon. The reduction of samples is rather surprising in

view of the stability diagram of the $Cu/Cu_2O/CuO$ system calculated by thermodynamical considerations and shown in figure 10. In this diagram we see that at temperatures in the vicinity of $390^{\circ}C$, the Cu_2O system is well within the stability region up to very low oxygen pressure. Fortin (16) has come across the same problem in his investigations. He has suggested that this could be due to the contamination of the samples and surroundings with organic matter which cause reduction and render the stability diagram meaningless.

The conductivity and activation energies of the samples depended strongly upon the thermal history of the samples. Values of activation energies and resistances for different samples heated at different temperatures are shown in table I. The resistance measurements during heating were made under varying pressure (10^{-7} mm to 10^{-4} mm of Hg), due to the release of occluded and adsorbed gases during heating. It was observed that a discontinuity in slope of the conductivity curves occurs near about $80^{\circ}C$ during heating for all samples (figures 11, 13). Resistances measured during cooling from $950^{\circ}C$ was under gradually improving vacuum (10^{-4} mm to 10^{-7} mm of Hg).

A glance at table 1 shows that the different samples do not have one to one correspondence to each other either in resistance or in activation energies in spite of the fact

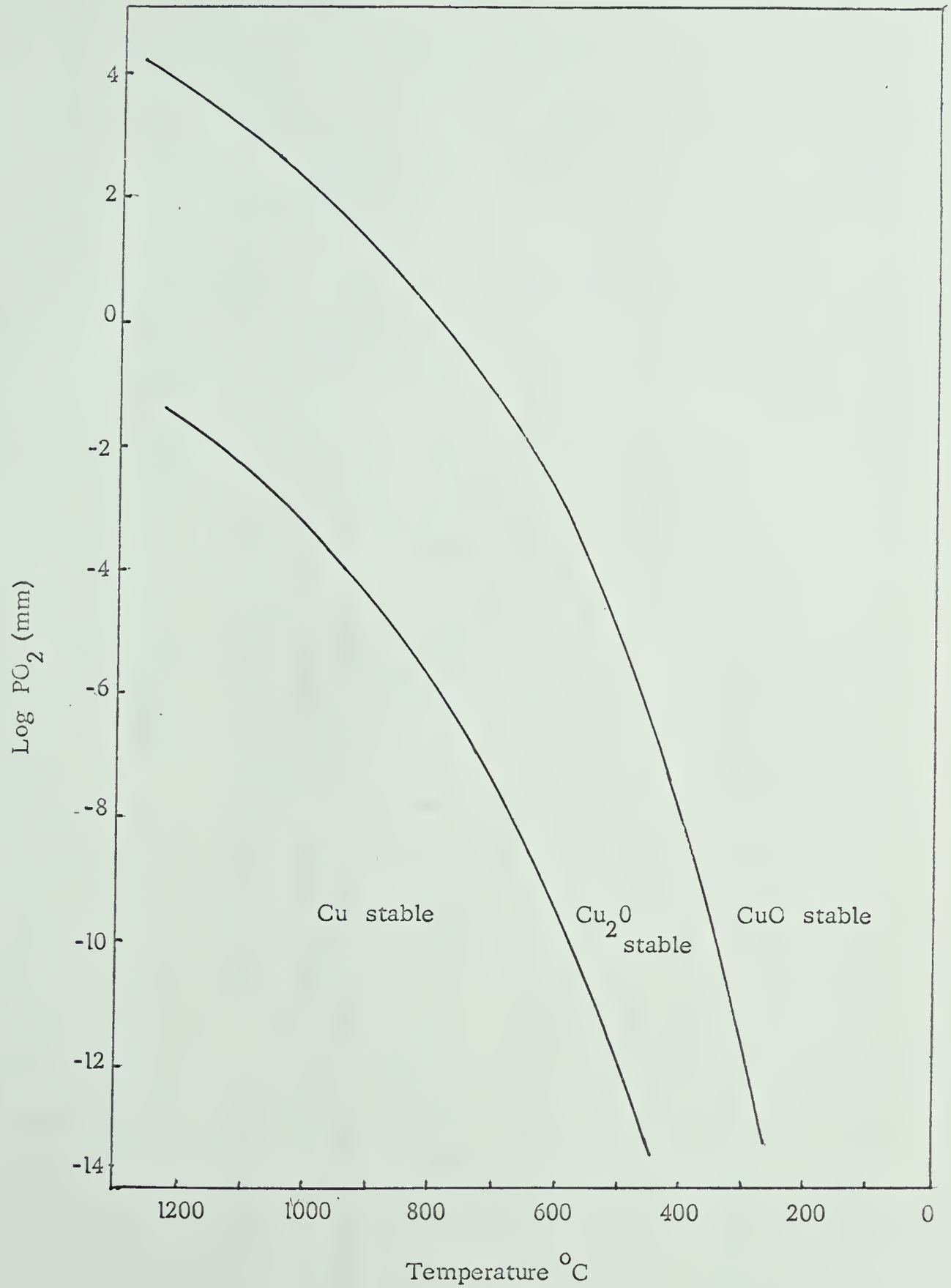

Figure 10. Stability diagram for the $Cu/Cu_2O/CuO$ system.

Table I

Sample Number	Before heating		After heating up to 150°C		After heating bet. 200-250°C		After heating up to 950°C	
	Activation energy	Resistance at room temp.	Activation energy	Resistance at room temp.	Activation energy	Resistance	Activation energy	Resistance
1	0.3 ev	2.1×10^7 Ω	.51, .44 ev	1.9×10^8 Ω	.66, .56, .26 ev	~10^8Ω		
2	0.27 ev	1.8×10^6 Ω	-	-	.67, .52, .22 ev	1.1×10^9	.79,.52 ev	1.5×10^9Ω
3 etched	.29 ev	3.1×10^7 Ω	-	-	.69, .59, .2 ev	6.5×10^8	-	-
4	.32,.24 ev	4.0×10^6 Ω	.37, .49 ev	~10^8 Ω				
4 etched	.32, .16 ev	6.5×10^5 Ω	.3, .43 ev	1.0×10^7 Ω	-	-	.82, .69 ev	1×10^{10}Ω

that they were prepared under identical conditions. However some of the behaviour is common between the samples. Heating the samples in vacuum (for a few hours to a day) increases the resistance by several orders of magnitude. For the samples heated to 950°C we get only two values of activation energies whereas for samples heated at lower temperature we have several. All the unheated samples on the other hand have activation energy in the vicinity of 0.3 ev. However, the values of activation energy of 0.79 ev and 0.82 ev, obtained in the temperature region where intrinsic conductivity in Cu_2O is believed to take place, is rather low. One usually obtains an activation energy of .9 to 1.0 ev for intrinsic conduction thereby giving a band gap of about 2.0 ev in Cu_2O. The low activation energy in our case may have been due to the absorption of oxygen by the sample during cooling as the vacuum was of the order of 10^{-4} mm of Hg. From conductivity measurements Fortin (16) has obtained activation energies as 0.3, 0.4, 0.6, 0.9 to 1.0 ev for similar crystals in this laboratory. McInnis (17) however, has obtained activation energies between 0.4 to 0.7 ev for extrinsic conductivity and 0.92 ev for intrinsic conductivity for similar crystals. From photoconductivity measurements, McInnis has obtained activation energy of 0.52 ev and 0.8 ev. The conductivity curves for sample #4 upon which the results of exciton studies are reported here, are shown in figures 11 to 15.

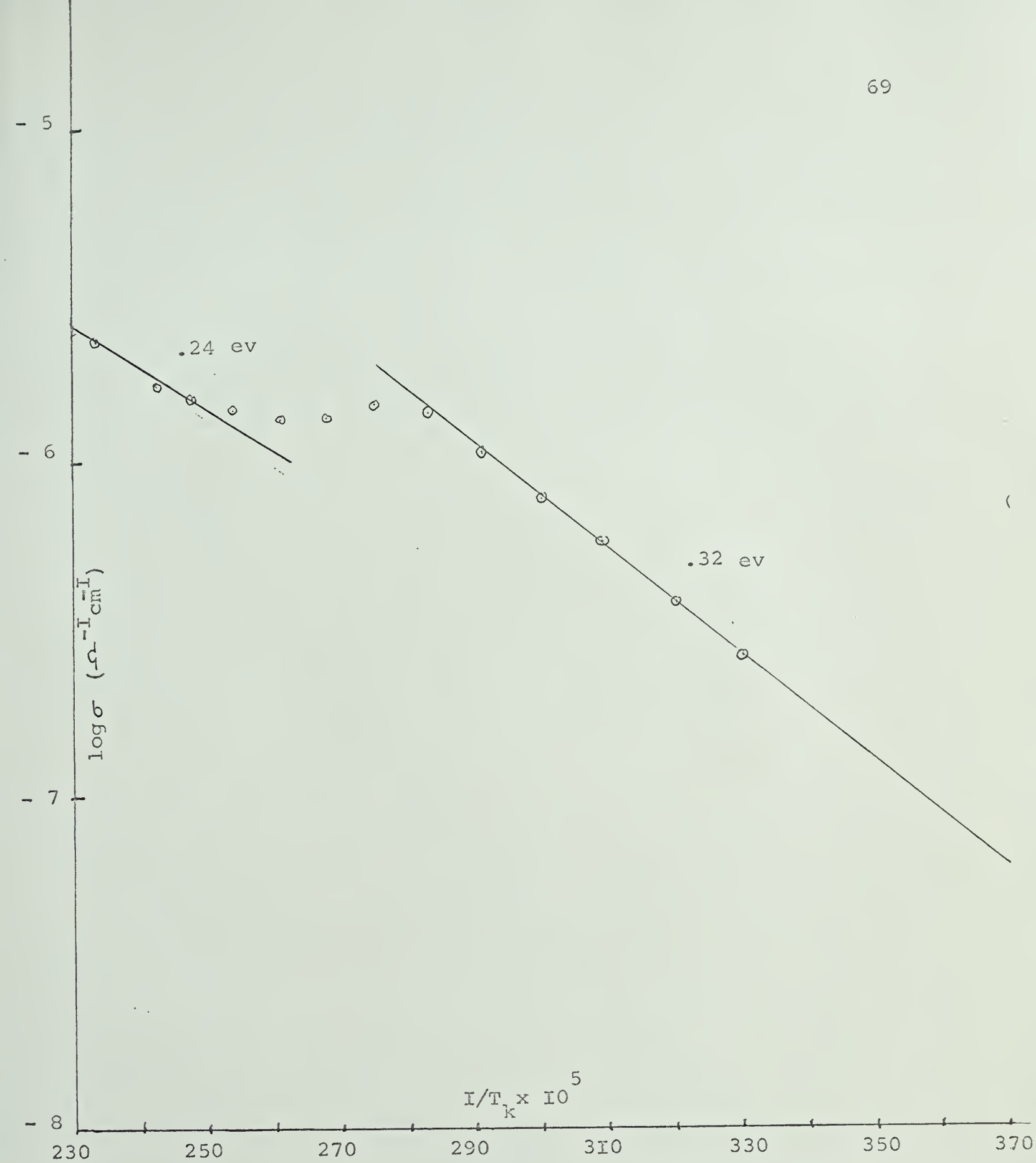

Figure II. log σ Vs I/T for unetched sample during heating to I50°C.

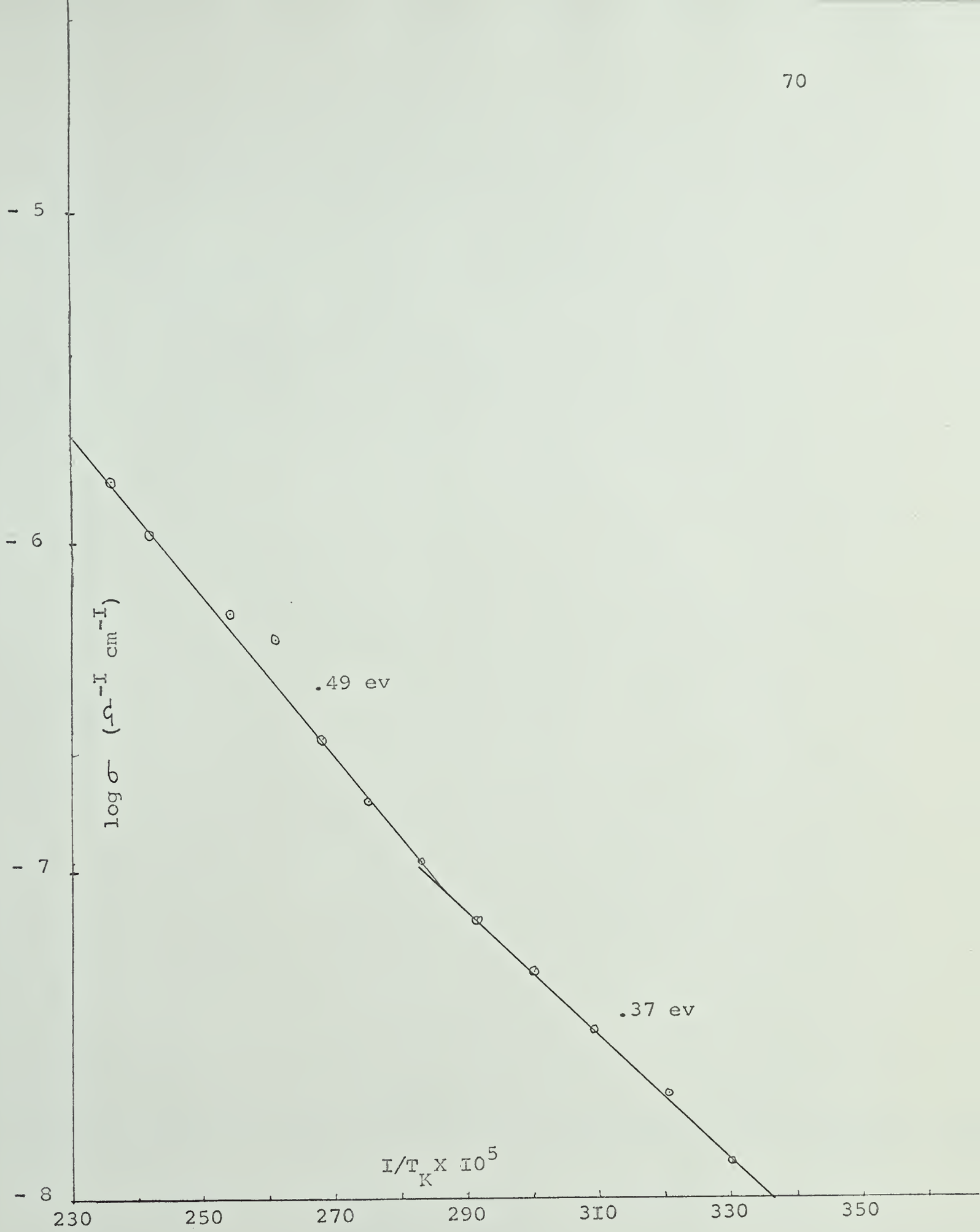

Figure I2. log σ vs I/T for unetched sample during cooling from I50° C.

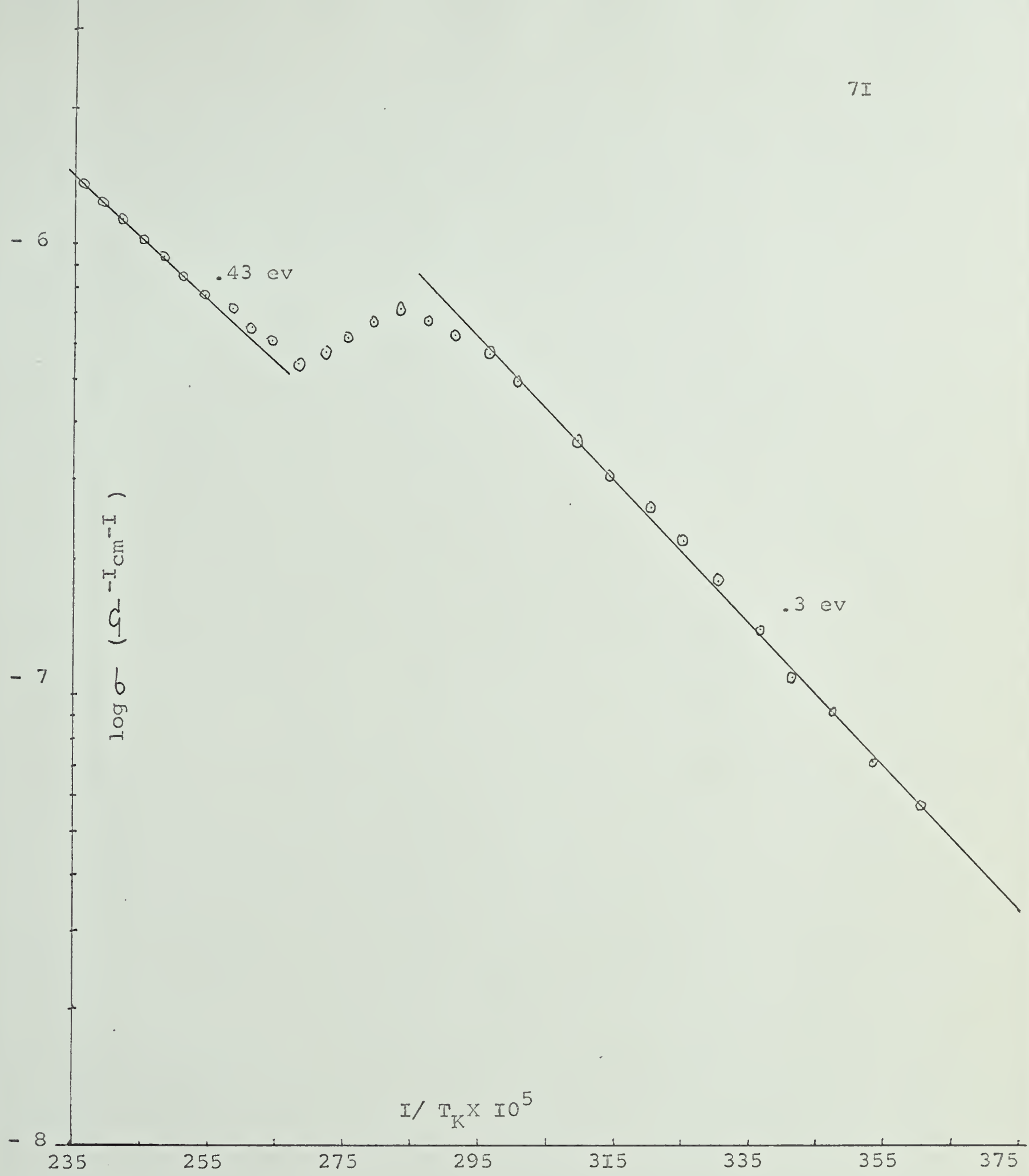

Figure I3. log σ vs I/T °K for etched sample during heating to I50° C.

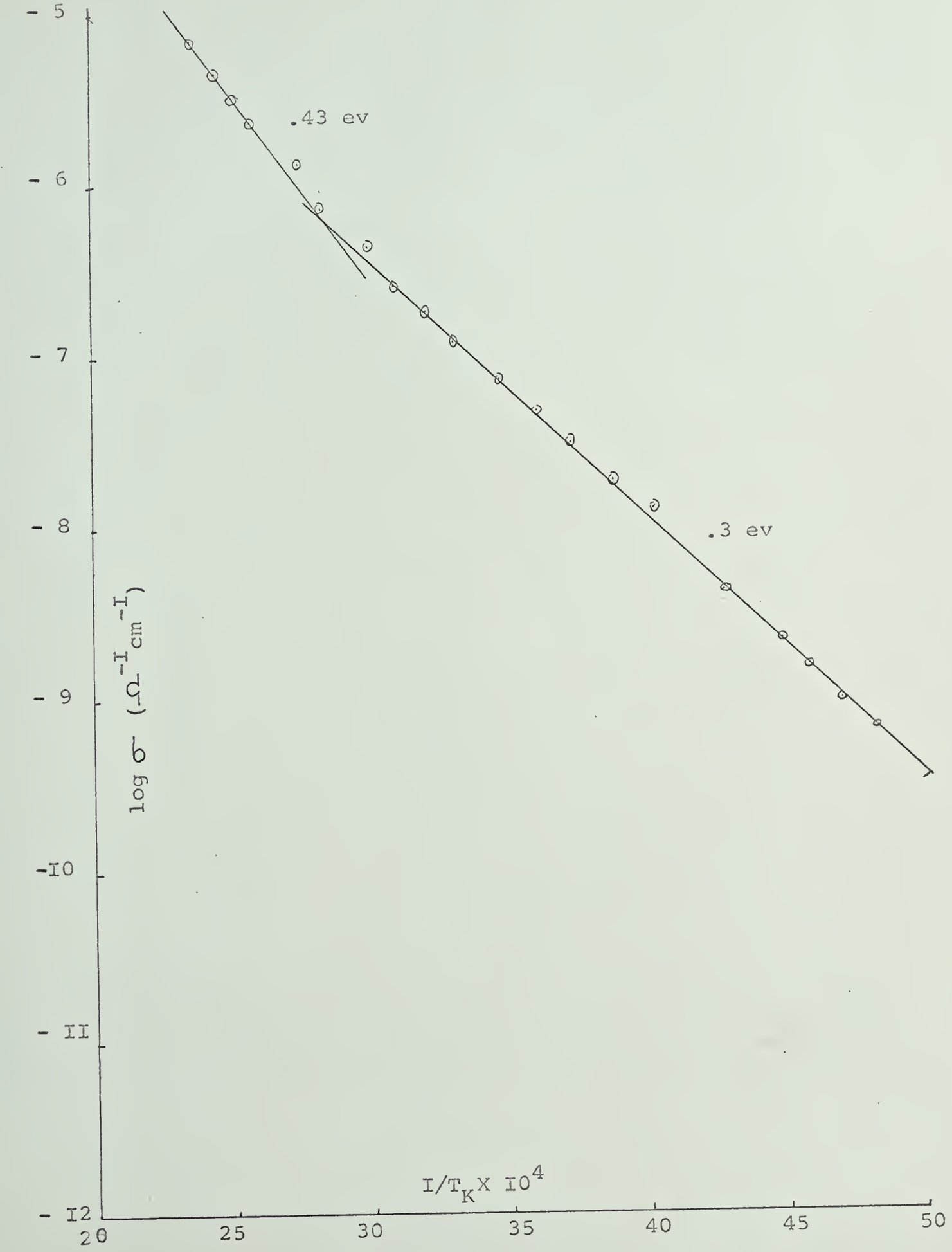

Figure I4. log σ vs I/T for etched sample during cooling from I50° C.

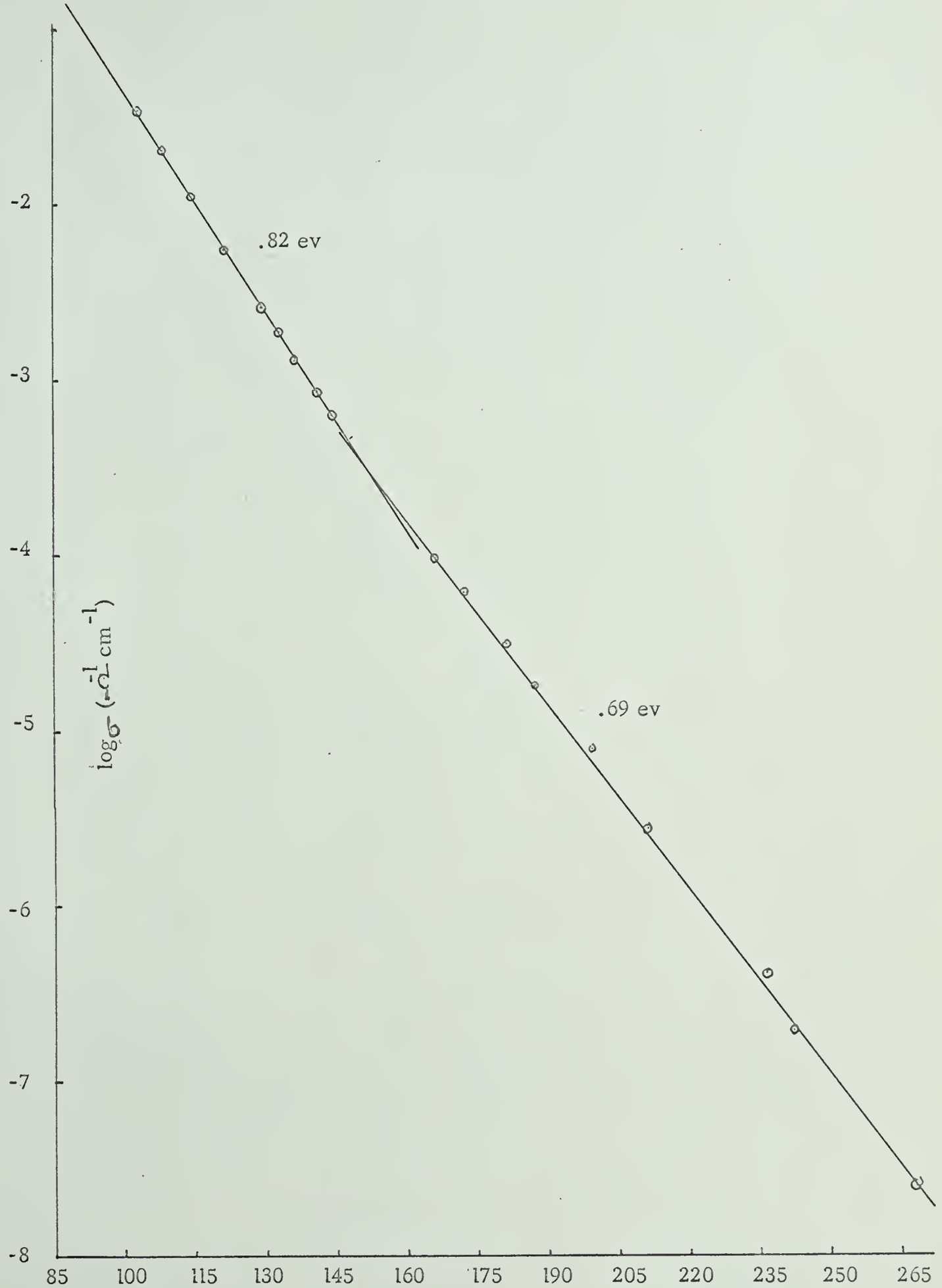

Figure 15(a). $\log\sigma$ vs $1/T$ for sample heated to 950°C in vacuum.

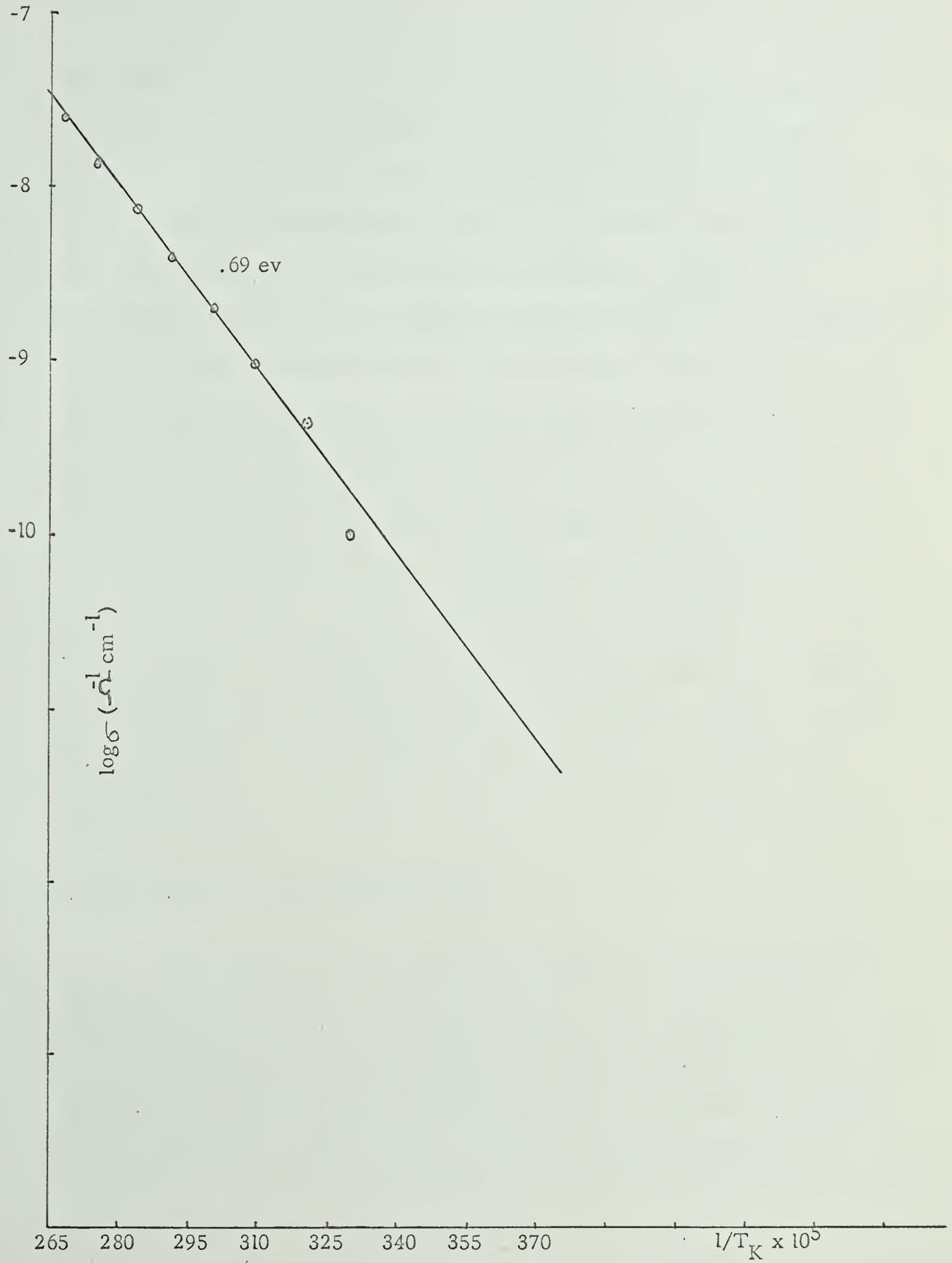

Figure 15(b). $\log \sigma$ vs 1/T for sample heated to 950°C in vacuum.

The impurity levels in Cu_2O have usually been attributed to the presence of excess oxygen in the lattice or to copper vacancies. To date all Hall effect measurements in Cu_2O (12, 16, 42, 41) have shown p-type conductivity which suggest that these impurity levels act as acceptors. Fortin by measuring the Hall constant for similar crystals has suggested a number of acceptor levels in the forbidden gap.

The conductivity increases when the sample is exposed to air but decreases when heated in vacuum. This has been explained by assuming that oxygen is absorbed at the surface of crystal which produces low lying acceptor levels which are removed after heating. According to Suchet, however, the oxygen absorbed is not removed by heating of the sample but is redistributed to a certain extent throughout the crystal. This explanation seems very plausible in our case.

4.2. Exciton induced photoconductivity.

The observations for photoconductivity in the green, yellow and red regions of excitons were taken with sample no. 4, but subjecting it to different surface and heat treatments. Photoconductivity curves were initially obtained with the unheated sample with a natural surface and then by

annealing the sample at 150°C in vacuum. The sample was exposed to air and the surface was then etched with dilute nitric acid (1 part concentrated nitric acid + 4 parts of water by volume). Photoresponse was then taken with this sample and again after heating it at 150°C and 950°C in vacuum. The electrical conductivities of the sample treated in such a way has already been summarized in Table I. Several photoconductivity vs. wavelength runs were made after each treatment. Usually the first response curve was a little different from the subsequent ones which reproduced well within experimental errors. These variations in subsequent observations could be attributed to several reasons, the most important one being due to inherent noise in the sample at liquid nitrogen temperature and also due to vibrations produced by the bubbling of liquid nitrogen in the dewar and the mechanical vibrations of floors, etc. Observations were all taken at night when the mechanical vibrations were considerably less. The response curves shown in figures 16 to 22 were found to be typical for the sample.

In order to find whether negative photoeffect as observed by Coret and Nikitine (37) and Pastrnyak and Timov (38) could be observed for our samples as well. Variable electric field was applied (up to 2 Kv/cm) to the crystal in all the above cases and the photoresponse curves were obtained by

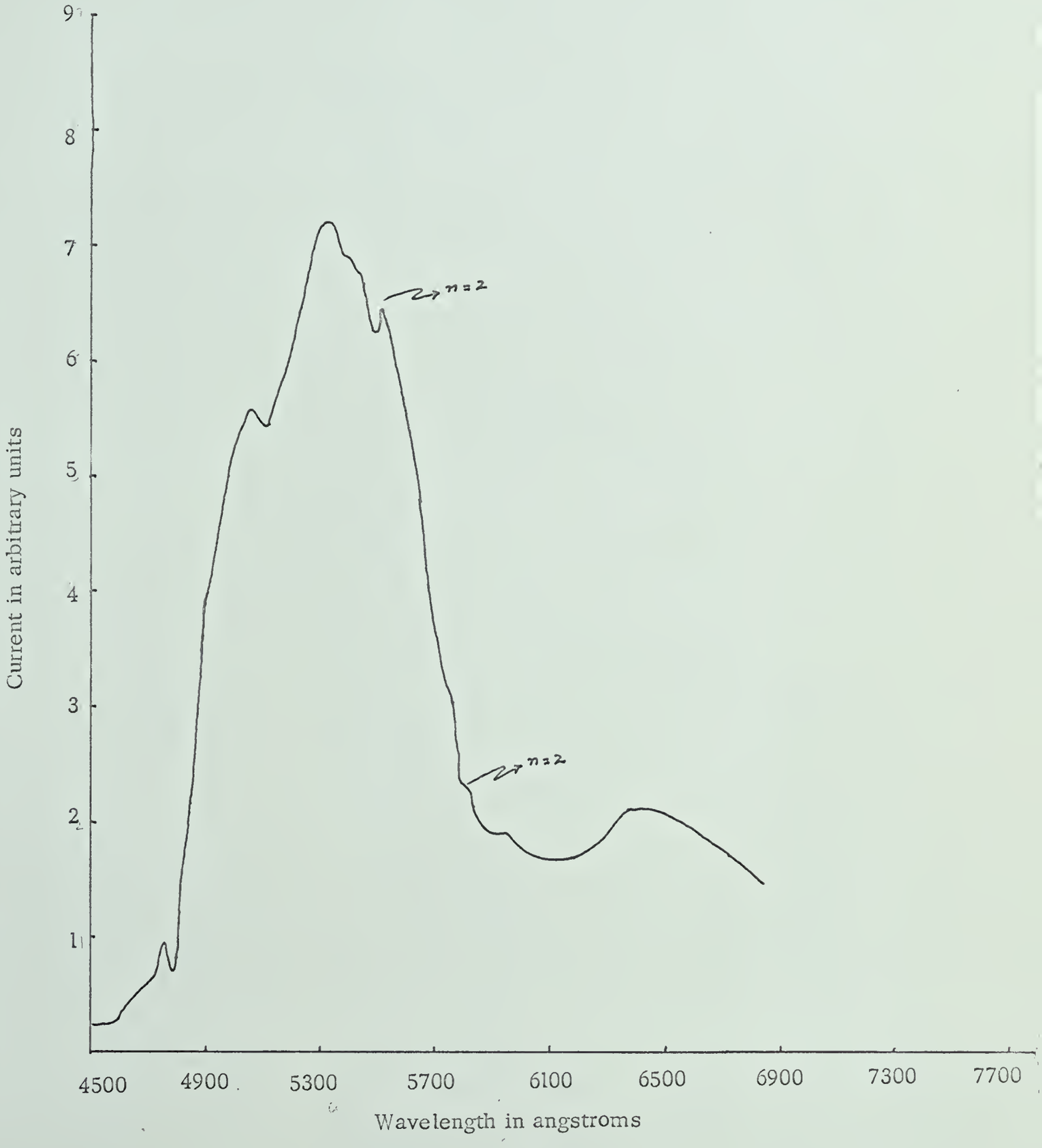

Figure 16. Response curve for unetched and unheated sample.

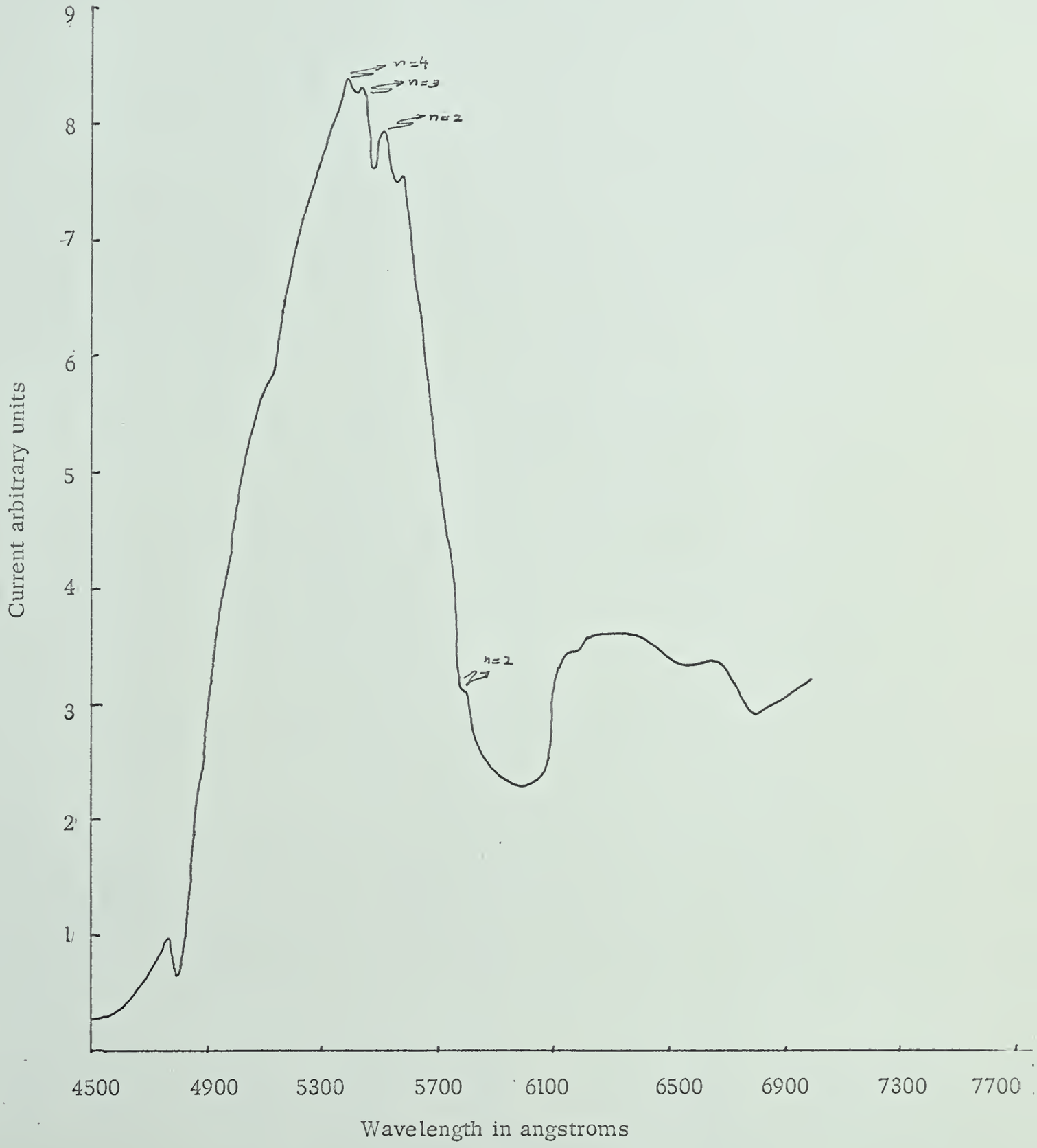

Figure 17. Response curve for unetched sample and heated to 150°C in vacuum.

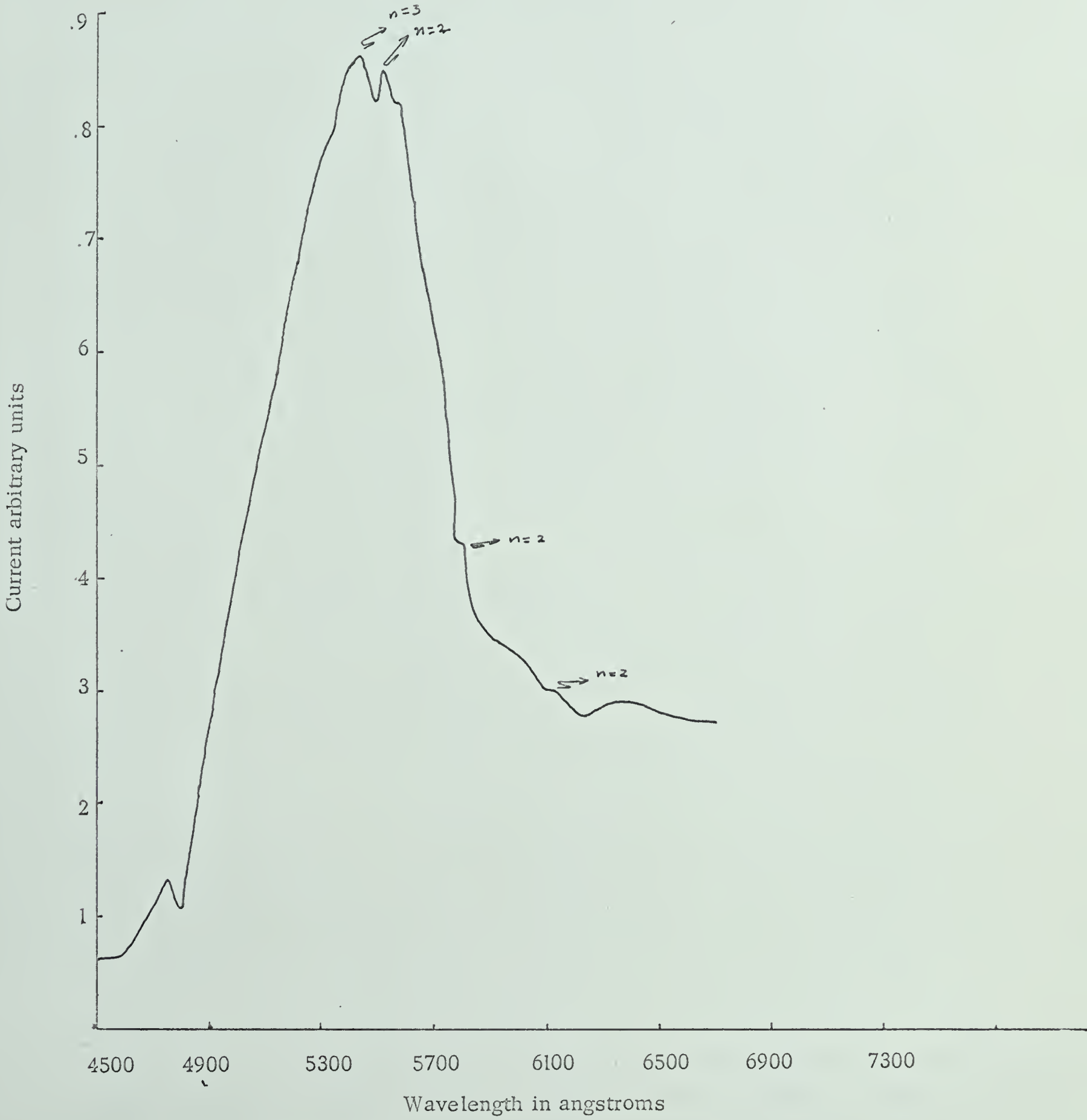

Figure 18. Response curve for etched and unheated sample.

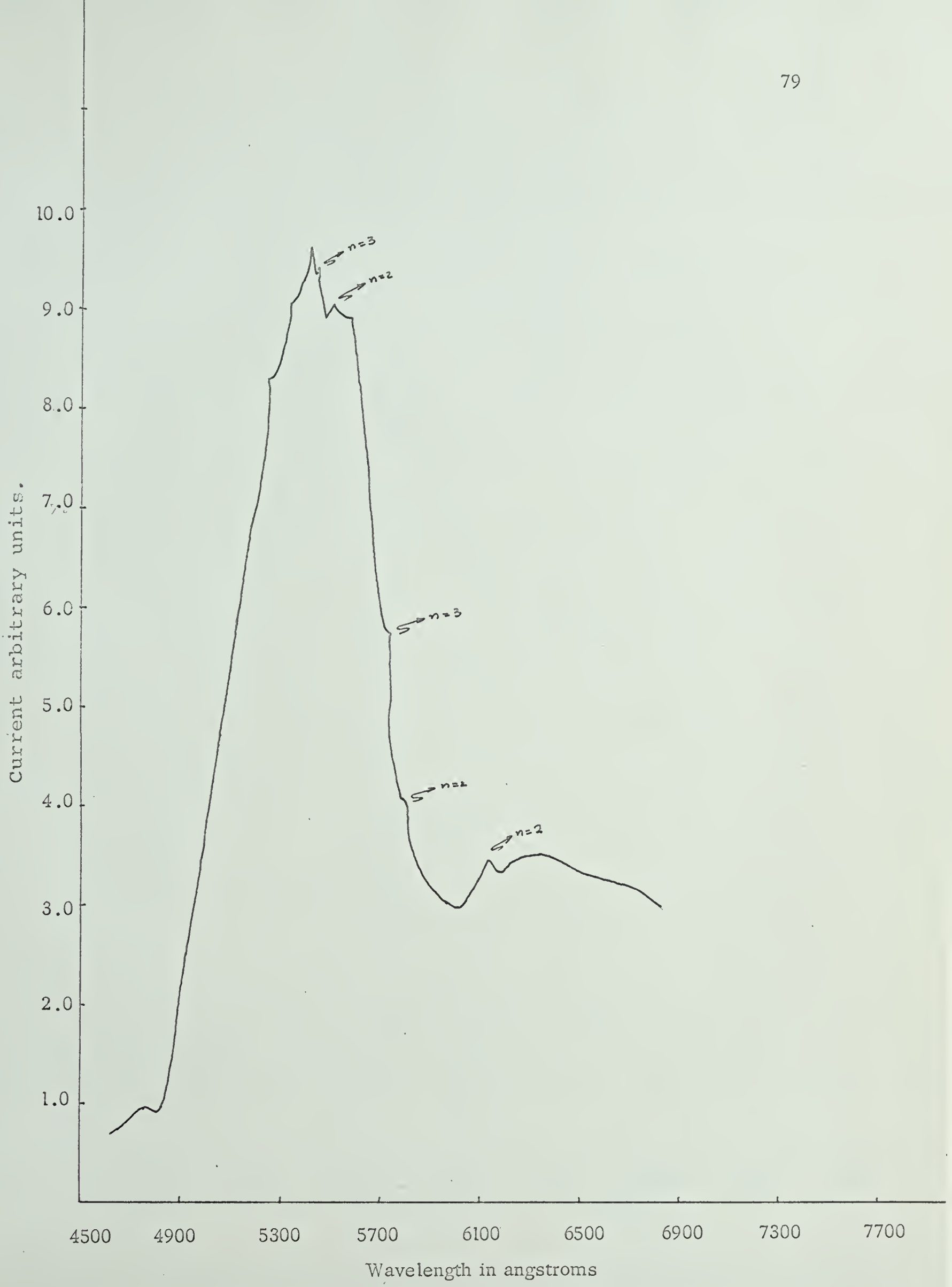

Figure 19. Response curve for sample heated to 150°C in vacuum. (etched)

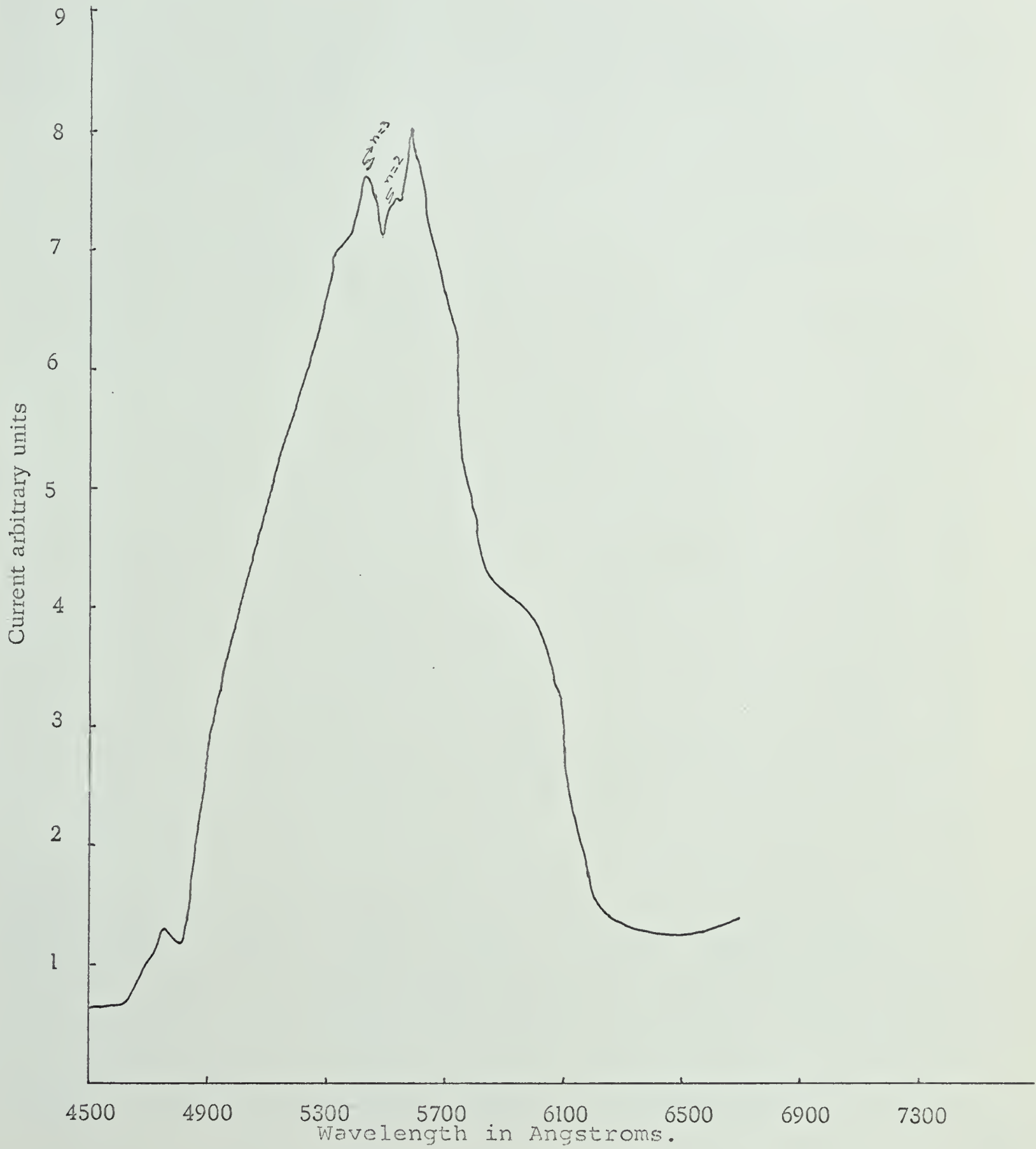

Figure 20. Response curve for etched sample heated to 950°C in vacuum.

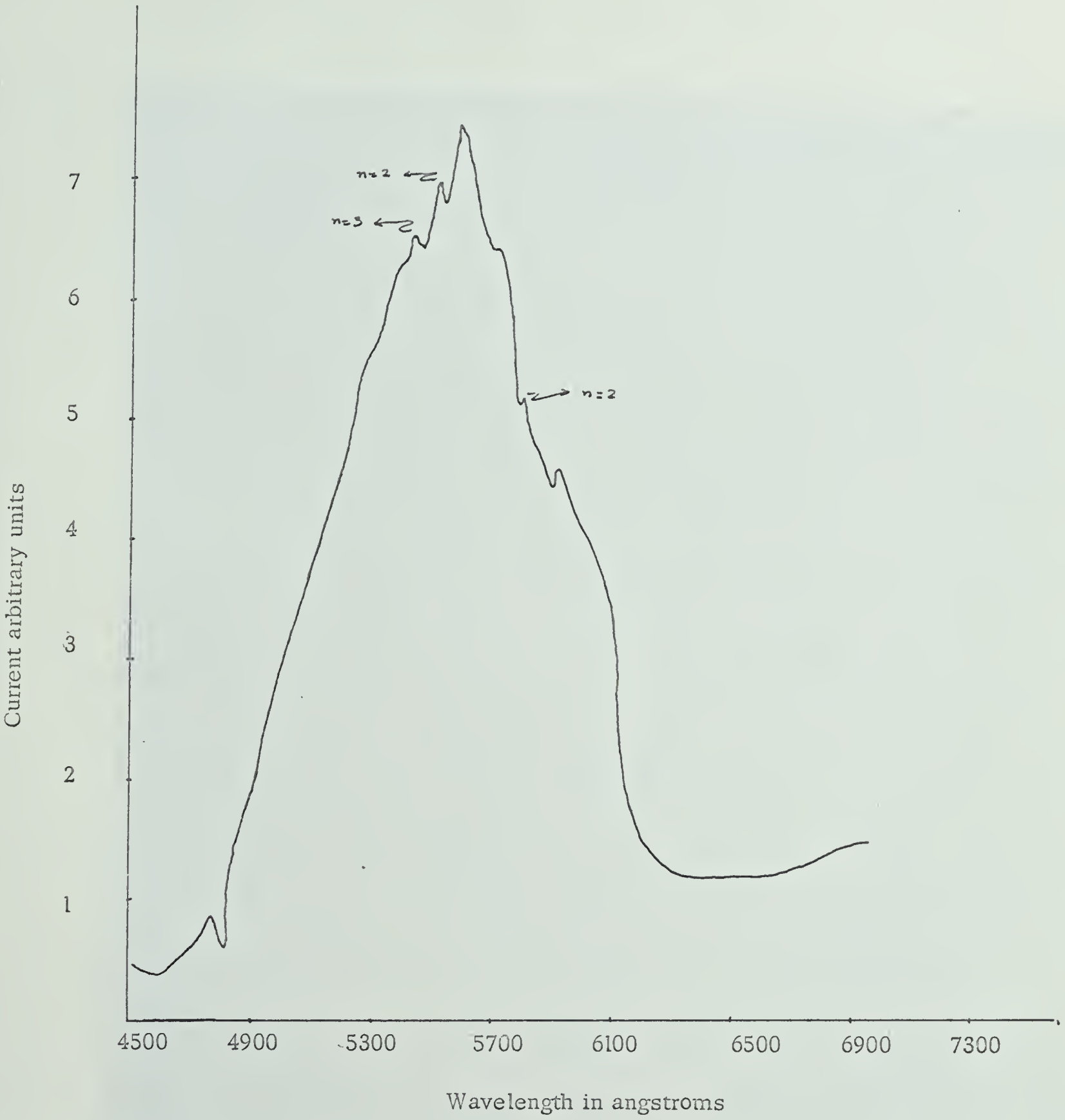

Figure 21. Response curve for etched sample heated at 150°C in air.

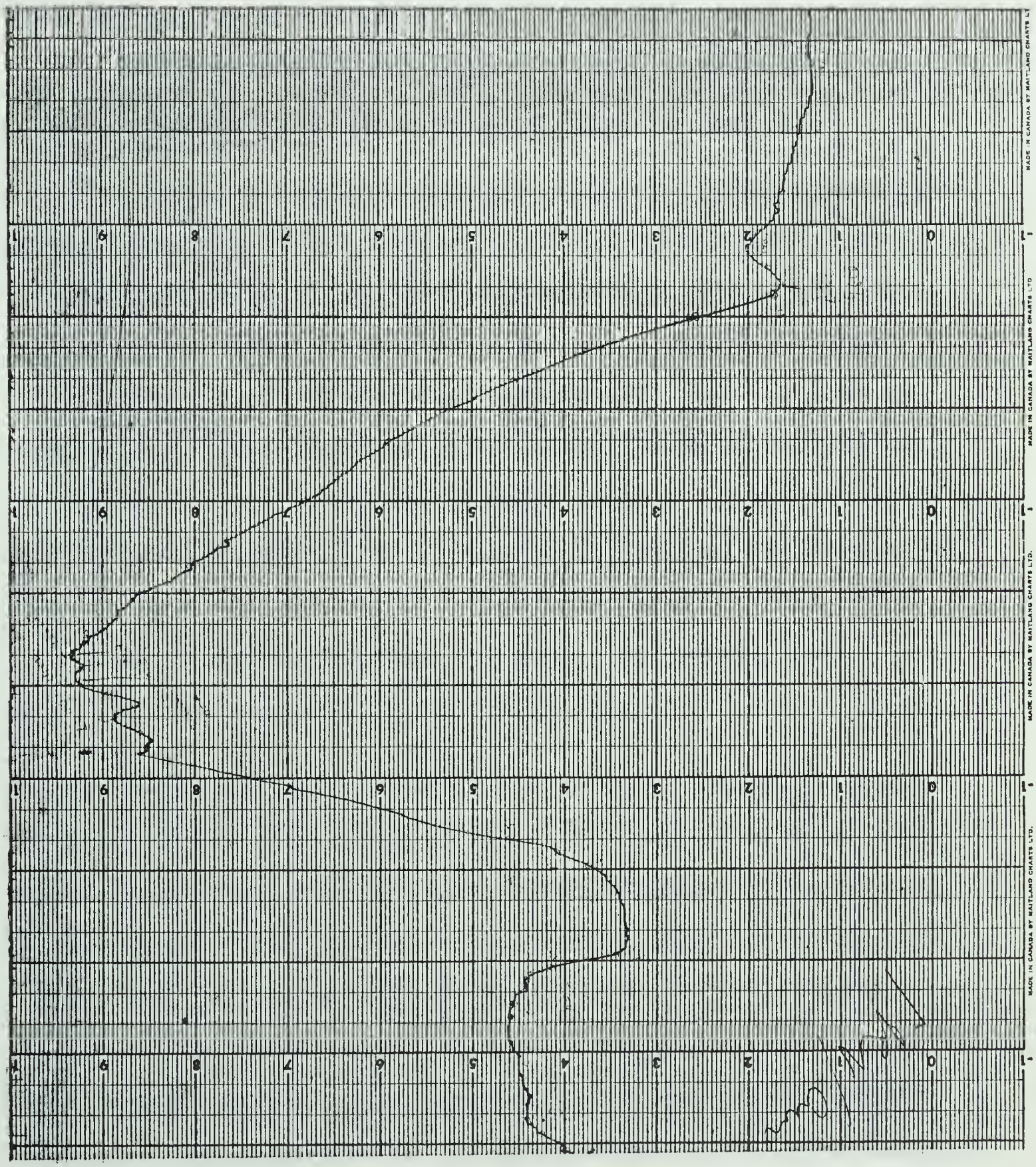

Figure 22. Reproduction of the response curve obtained for unetched sample heated to 150°C in vacuum on the chart recorder.

scanning the whole visible spectrum. Several observations were taken here also for reproducibility. These observations also served for the study of the effect of electric field on the exciton induced photoconductivity. The results of these investigations could be summarized as follows:

1. For unheated samples having considerable water vapour and oxygen absorbed at the surface, we obtained a relative maximum of photoconductivity at 5510 corresponding to the line n = 2 in the green excitonic series. The structure due to the other lines in the series was unresolved. Another peak at about 5800 A^{o} was observed which coincided with the position of the line n = 2 in yellow exciton series. A minimum of photoconductivity at 4790 A^{o} can be correlated to the exciton line in blue exciton region. The other peak at 5060 A^{o} in figure 16 vanished after the sample is heated. No structure was observed in the red region.

2. When the sample was heated for about 30 hours in vacuum at about 150^{o}C, the sample became a bit more sensitive for longer wavelength than for the unheated sample and the maximum of curve shifts towards longer wavelength. The heated sample also became more photosensitive than the unheated sample in the whole region of spectrum and as seen in Table I its dark conductivity at room temperature had decreased after heating. The structure in the photoconductivity curve becomes

more resolved. We observe maxima of photoconductivity in the green exciton lines for n = 2, 3, 4. A peak for the yellow n = 2 exciton line is observed at 5790 A^{o} but here the peak is not well resolved. Some structure in photoconductivity is observed in red region of spectrum at 6140 A^{o} at the position of n = 2 exciton line in red. An extra peak is observed at about 5575 A^{o} which could not be correlated to any known exciton line. We still get a minimum of photoconductivity corresponding to the blue exciton line at about 4790 A^{o}.

3. Exposing the sample to air and etching the surface of the crystal did not profoundly change the nature of the photoresponse of the sample. We got two peaks for the green exciton series and also one peak for yellow as well as red. Except for the broadening of peak the photoconductivity curve resembles the previous two curves. The extra peak observed in the last case is also present here.

4. With the etched sample heated to 150^{o} in vacuum the response is similar to the unheated sample except that the sample becomes more photosensitive and the room temperature conductivity is lower as compared to the samples exposed to air. However, the structure in blue region becomes less pronounced whereas the structure for the red exciton line becomes more

pronounced. In the yellow region instead of one peak we now get another peak at 5730 A^{o} which corresponds to n = 3 line in the yellow series.

5. For samples heated up to 950^{o} in vacuum and then cooled the peak of photoconductivity response curve moves still further towards longer wavelength. The shape of the response curve is modified towards yellow and red region of spectrum and the fine structure of the curve is lost in these regions. In green region also the peak corresponding to n = 2 line becomes very indistinct as compared to the peak corresponding to the n = 3 line which becomes more pronounced. Thus in all regions of spectrum except blue the excitonic peaks become less pronounced than in the samples heated at 150^{o}C.

For samples heated to 150^{o}C in air for about one day we observe the same shift of spectrum towards the longer wavelength as for sample heated to 950^{o}C in vacuum compared to unheated samples. But here the peaks due to excitons are more pronounced in all regions except red where no structure is observed.

The effect of electric field on excitons is not very pronounced up to a field of 2 Kv/cm. However, for higher electric fields the photoconductivity in the lines for higher

quantum number in green exciton lines seems to be quenched. This phenomenon is more pronounced in the heated samples.

The effects observed in photoconductivity in exciton lines do not agree with the observations obtained by others in one important way and that is: the maxima or minima of photoconductivity does not vary with the annealing of the samples. Also, we could not obtain any structure in photoconductivity in the violet region of the spectrum. It was assumed that heating the sample changes the surface condition in the sample by either removing impurities or adding some (e.g. formation of CuO) thereby changing the maxima of photoconductivity to minima or vice versa. Coret and Nikitine (37) [redacted] have observed that the maxima of the photoconductivity for the blue exciton line becomes a minimum after heat treating the sample at 150°C in air. In our case though the background photoconductivity upon which the excitonic photoconductivity peaks are superimposed is appreciably changed, the maxima or minima of photoconductivity do not change. Also, Coret and Nikitine (37), Pastrnyak and Timov (38) have observed negative photoeffect at high fields. We could not observe any negative photoconductivity in the sample up to a field of 2 Kv/cm. However, these effects have been observed in multicrystalline solids and explained on the basis of the existance of traps at the intercrystalline boundaries

of the crystallites composing the crystals. Therefore, our observations confirm the earlier suggestion by Coret and Nikitine (37) that negative photoeffect should not be observed in monocrystalline solids.

In all the samples studied we could not get any structure in photoconductivity curve near about 123°K, which was the temperature attainable in vacuum with our set up prior to the leakage of helium as a heat exchanger. Apfel and Portis (9) could however obtain structure in photoconductivity due to excitons up to a temperature as high as 170°K in multicrystalline samples. Optical absorption spectra in Cu_2O also have shown structure in this temperature range (40).

The disagreement between our results and results obtained by other investigators can be attributed to the nature of the sample itself. It is well known that the electrical properties in Cu_2O depends strongly upon many factors such as mode of preparation, impurity contents, nature of the surface, etc. Multi and polycrystalline samples also differ in electrical properties from monocrystalline samples. All the experiments performed so far on the exciton induced photoconductivity in Cu_2O has been performed either on multi and polycrystalline samples or impure crystals of Cu_2O greatly. Observations were taken either in vacuum (9, 37, 4)

or dipping the crystals directly in liquid nitrogen (8, 38). The mode of preparation for these crystals was such that their dark conductivities at room temperature and liquid nitrogen temperature was much higher as compared to ours. Coret and Nikitine (37) had a resistivity of only 0.5×10^{-9} Ω-cm at liquid air temperature. The samples used by Apfel and Portis (9) had room temperature resistivity of 5×10^{3} Ω-cm and a resistivity of 3×10^{10} Ω-cm at 100°K. The resistivity of our samples at its worst was 7.0×10^{5} Ω and as high as $\sim 10^{10}$ Ω-cm at room temperature. Unfortunately not much information is given by the above authors about the electrical conductivity and activation energies of the samples used in the experiments and the subsequent changes brought about in them by surface and heat treatment. However, the difference between our samples and samples used by other investigators can be found in the mode of their preparation. The cooling of our samples in vacuum, as described, after oxidation and annealing pure Cu_2O samples were obtained which were at the oxygen poor limit of their composition range. These samples will be close to stoichiometry which is responsible for their high resistivity. Most of the authors however quench their samples from high temperature. It will not be very unreasonable to assume that the quenching of samples from high temperatures will produce [redacted] surface defects acting subsequently

as acceptor levels of low activation energy. Our samples will therefore differ both in nature of volume as well as the surface of the crystals. Only experimental data for photoconductivity of such samples, to our knowledge, is the work of McInnis in this laboratory. Our sample #4 was rather poor as compared to McInnis' crystal in the sense that we obtain lower values of band gap which may be the consequence of oxygen absorbed by our sample when heated to 950°C as discussed earlier. If defects and impurities play important role in the breaking up of excitons, it will not be very unreasonable to expect variations in our results as compared to the results obtained by other investigators. Though dark conductivity and activation energies of our sample change by heating it seems that they do not seem to rpoduce any modifications in the nature of maxima or minima of exciton induced photoconductivity. And this is also true of etching of the crystal surface.

4.3. CONCLUSIONS

The results obtained above can be explained, at least qualitatively, on the basis of the mechanism annihilation or dissociation. These explanations however cannot be unique. This is due to the fact that the phenomena of extrinsic photoconductivity in Cu_2O itself is rather complex and defies an unique and straightforward explanation.

The increase in photoconductivity in exciton lines observed in yellow and green region of spectrum can be explained on the basis of the assumption of breaking up of excitons on defects and/or impurities. The exciton once formed breaks up into holes and electrons. Because Cu_2O is a p-type semiconductor and we get an increase in photoconductivity in green and yellow exciton lines, we can assume that there exists electron traps in the sample. These traps capture the freed electron of the exciton. The hole is thereby left which increases the hole concentration and thereby causing the increase in photoconductivity. Because we do not get change from the maxima to minima of photoconductivity in exciton lines due to surface and heat treatments, we can assume that the nature of electron trap is not changed by these treatments. The disappearance of structure in red region after heating the sample at high temperatures shows that these structures are probably not due to excitons. The appearance of minimum in blue region can be at least partly explained by Devore's effect discussed earlier.

From our observations we can conclude that the type of samples used where the defects are minimum we should not expect to see any change by the nature of exciton induced photoconductivity different surface and heat treatments provided

the surface is clean enough. From the absence of structure at 123°K we obtain a hint that excitons play a relatively unimportant role in photoconductivity especially in pure crystals. However, a thorough investigation is required to arrive at a definite conclusion. Such experiments should be performed on crystals of our purity but on different samples of the same production series as well as others. A study of the type of defect in our crystals will also go a long way in explaining the phenomena more clearly.

REFERENCES

1. Frenkel, J. Phys. Rev. 37, 17, 1276 (1931).
2. Peierls, R. Ann. Physik 13, 905 (1932).
3. Wannier, G. H. Phys. Rev. 52, 191 (1937).
4. Mott, N. F. Proc. Roy. Soc. (London) 167, 384 (1938).
5. Gross, E. F. and Karryev DAN SSSR 84, 471 (1952).
6. Hayashi, M. J. Fac. Sci. Hokkaido Univ. 4, 107 (1952).
7. Gross, Kaplyanskii and Novikov. Soviet Phys. Tech. Phys. 1, 674, 900 (1957).
8. Gross, E.F., and Pastrnyak, Soviet Phys. Solid State 1, 143, 758 (1959).
9. Apfel, J.H. and Portis, A.M., J. Phys. Chem. Solids 15, 33 (1960).
10. Toth, R.S., Kilkson, R., Trivich, D., Phys. Rev., 122, 482 (1961).
    J. Appl. Phys., 31, 1117 (1960).
11. Juse, W.P., and Kurtschatov, B.W. Phys. Z. Sowjet, 2, 453 (1933).
12. Engelhard, E., Ann. Phys., Lpz. 17, 501 (1933).
13. Anderson, J.S. and Greenwood, N.W., Proc. Roy. Soc. 215 A, 353 (1952).
14. Böttger, O., Ann. d. Phys., 10, 232 (1952).
15. O'Keeffe, M. and Moore, W.J., J. Chem. Phys. 35, 1324 (1961).
16. Fortin, E.R., Ph.D. Thesis, University of Alberta (1965).
17. McInnis, B.C., M.Sc. Thesis, University of Alberta (1963).
18. Moss, T.S., Photoconductivity in elements. New York Academic Press (1952).

I9. DeVore, H.B., Phys. Rev. 102, 86 (1956).

20. Elliot, R.J., Phys. Rev. 108, 1402 (1957).

21. Nikitine, S. J. Chem. Phys. 55, 621 (1958).
Phil. Mag. 4, 1 (1959).
J. Phys. Chem. Solids 8, 190 (1959)

Nikitine, S., Reiss, R. and Sieskind, M.C.R.,Acad. Sci. Paris 246, 3439 (1958).

22. Hayashi, M., and Katzuki, K., J. Phys. Soc. Japan 5,380 (1950) 7,599 (1952)

23. Nikitine, S., Perny, G., and Sieskind, M., J. Phys. Radium 15, S 18 (1954); C.R. Acad. Sci. Paris, 238, 67 (1954).

24. Dexter, D.L. Phys. Rev. 83, 435 (1951).

25. Overhauser, A.W. Phys. Rev. 101, 1702 (1956).

26. Hayashi, M. Prog. of Theo. Phys., Suppl. 12, 160 (1959).

27. Nikitine, S. Prog. in Semiconductors, Vol. 6, 297 (1961).

28. Grun, J.B., Sieskind, M., and Nikitine S., J. Phys. Chem. Solids 19, 189 (1961)

29. Gross, E.F., Adv. Phys. Sci., Moscow 63, 575 (1957).

30. Brymner, R. and Steckelmacher, W., J. Sci. Instr. 36, 278 (1959).

31. Lipnik, A.A., Soviet Phys. Solid State 3, 1683 (1962).

32. Goodman, B. and Oen, O.S., Phys. Chem. Solids 8, 291 (1959).

33. Haken, H., Halbleiter Probleme 4 (1958).

34. Choi, S.I., and Rice, S.A., Phys. Rev. Letters 8, 410 (1962).

35. Apker, L., and Taft, E., Phys. Rev. 79, 964 (1950); 81, 698 (1951).

36. Philipp, H.R., and Taft, E.A., Phys. Rev. 106, 671 (1957).

37. Coret, A. and Nikitine, S., J. Phys. Radium 24, 581 (1963).

38. Pastrnyak, I., and Timov, R.A., Soviet Phys. Solid State 3, 627 (1961).

39. Elliot, R.J., Phys. Rev. 124, 340 (1961).

40. Nikitine, S., Sieskind, M., and Perny, G., C.R. Acad. Sci. Paris 238,1987 (1954).

41. Nieke, H. Ann. d. Physik 12, 297 (1953).

42. Wright, M., Ph.D. Thesis, Wayne State University, Detroit, Michigan (1962)